Dynamics of lattice kinks

P.G. Kevrekidis * and M.I. Weinstein †

February 11, 2000

Abstract

We consider a class of Hamiltonian nonlinear wave equations governing a field defined on a spatially discrete one dimensional lattice, with discreteness parameter, $d = h^{-1}$, where $h > 0$ is the lattice spacing. The specific cases we consider in detail are the discrete sine-Gordon (SG) and discrete ϕ^4 models. For finite d and in the continuum limit ($d \to \infty$) these equations have static kink-like (heteroclinic) states which are stable. In contrast to the continuum case, due to the breaking of Lorentz invariance, discrete kinks cannot be "Lorentz boosted" to obtain traveling discrete kinks. Peyrard and Kruskal pioneered the study of how a kink, initially propagating in the lattice dynamically adjusts in the absence of an available family of traveling kinks. We study in detail the final stages of the discrete kink's evolution during which it is pinned to a specified lattice site (equilibrium position in the Peierls-Nabarro barrier). We find:
(i) for d sufficiently large (sufficiently small lattice spacing), the state of the system approaches an asymptotically stable ground state static kink (centered between lattice sites).
(ii) for d sufficiently small $d < d_*$ the static kink bifurcates to one or more time periodic states. For the discrete ϕ^4 we have: wobbling kinks which have the same spatial symmetry as the static kink as well as "g-wobblers" and "e-wobblers", which have different spatial symmetry. In the discrete sine-Gordon case, the "e-wobbler" has the spatial symmetry of the kink whereas the "g-wobbler" has the opposite one. These time-periodic states may be regarded as a class of discrete breather / topological defect states; they are spatially localized and time periodic oscillations mounted on a static kink background.

The large time limit of solutions with initial data near a kink is marked by damped oscillation about one of these two types of asymptotic states. In case (i) we compute the characteristics of the damped oscillation (frequency and d- dependent rate of decay). In case (ii) we prove the existence of, and give analytical and numerical evidence for the asymptotic stability of wobbling solutions.

*Department of Physics and Astronomy, Rutgers University, Piscataway, NJ 08854-8019 USA

†Mathematical Sciences Research, Bell Laboratories - Lucent Technologies, and Department of Mathematics, University of Michigan - Ann Arbor, 600 Mountain Avenue, Murray Hill, NJ 07974-0636 USA

The mechanism for decay is the radiation of excess energy, stored in *internal modes*, away from the kink core to infinity. This process is studied in detail using general techniques of scattering theory and normal forms. In particular, we derive a *dispersive normal form*, from which one can anticipate the character of the dynamics. The methods we use are very general and are appropriate for the study of dynamical systems which may be viewed as a system of discrete oscillators (*e.g.* kink together with its *internal modes*) coupled to a field (*e.g.* dispersive radiation or phonons). The approach is based on and extends an approach of one of the authors (MIW) and A. Soffer in previous work. Changes in the character of the dynamics, as d varies, are manifested in topological changes in the phase portrait of the normal form. These changes are due to changes in the types of resonances which occur among the discrete internal modes and the continuum radiation modes, as d varies.

Though derived from a time-reversible dynamical system, this normal form has a dissipative character. The dissipation is of an internal nature, and corresponds to the transfer of energy from the discrete to continuum radiation modes. The coefficients which characterize the time scale of damping (or *lifetime* of the internal mode oscillations) are a nonlinear analogue of "Fermi's golden rule", which arises in the theory of spontaneous emission in quantum physics.

1 Introduction

Coherent structures, *e.g. kinks, solitary waves, vortices*, play a central role, as carriers of energy, in many physical systems. An understanding of their dynamical properties, *e.g.* stability, instability, metastability, is an important problem. While for many years Hamiltonian partial differential equations and their coherent structures, defined on a spatial continuum, have received a great deal of attention, there has been increasing interest in spatially discrete systems. Two important reasons are that (a) certain phenomenoma are intrinsically associated with discreteness and (b) numerical approximations of continuum systems involve the introduction of discreteness, which may lead to spurious numerical phenomena which require recognition. Some examples of the use of discrete systems in the modeling of physical phenomena are: the problem of dislocations propagating on a lattice (for which the Frenkel - Kontorova or discrete sine-Gordon model was originally proposed) [22, 1, 23], arrays of coupled Josephson junctions, [55, 25, 60], the problem of the local denaturation of the DNA double helix [61, 17, 19, 18] and coupled optical waveguide arrays [21, 43].

A result of the many investigations of discrete systems over the last ten to fifteen years has been a recognition, mainly through numerical experiments and heuristic arguments, of the often sharp contrast in behavior between the dynamics of discrete systems and their continuum analogues. Some of these contrasts are easy to anticipate. For example, continuum systems modeling phenomena in a homogeneous environment are translation invariant in space, and may have further symmetry, *e.g.* Galilean or Lorentz invariance that enable one to construct traveling solutions from static solutions. The analogous discrete system is expected to lose these symmetries and therefore the existence of traveling wave solutions is now brought into question. A natural question concerns the propagation of energy in the lattice; *if one initializes the system with data which, for the continuum model would result in a coherent structure propagating through the continuum, what is the corresponding behavior for the energy distribution on intermediate and long times scales on the lattice? Does the system "find" a coherent structure to carry the energy? Does the energy get trapped or pinned?* In this paper we seek to obtain insight into these questions for a class of discrete nonlinear wave equations. The special cases we consider in detail are the discrete sine-Gordon (SG) and discrete ϕ^4 equations. The methods however are rather general and apply to systems which can be viewed as the interaction between a finite dimensional system of "oscillators" with an infinite-dimensional system governing a continuous spectrum of waves; see the further discussion below and in section 7.

The basic characteristics of the dynamics of coherent structures in discrete systems were systematically explored in a pioneering paper by Peyrard and Kruskal [48]; see also the contemporaneous papers [27, 47, 59]. Of particular relevance to our work are the more recent articles of Boesch, Willis and coworkers [59, 54, 8, 9, 11, 10]. In this work the discrete sine-Gordon equation is solved with kink-like initial data on the lattice. Observed is a rapid initial velocity adjustment of the kink, a quasi-steady state phase, resonances of the kink oscillations with phonons (continuous spectral modes) and the emission of radiation, which results in the kink's deceleration and eventual pinning in the Peierls-Nabarro (PN) potential. The final stage involves the relaxation to an asymptotic state, which is either a static or time-periodically "dressed" kink. In a rough sense, this is a result of the absence of a smooth family of traveling kink solutions due to broken Lorentz invariance. Insight into this process can be gleaned by studying the linearized spectrum about the kink.

An important feature of the discrete systems that makes them very different from their continuum analogues is the presence of additional neutral oscillatory modes in the spectrum of the linearization about the coherent structures. The sources of these *internal modes* are principally of two types; see for example [7, 34, 30, 31]. (1) The continuum system is translation invariant, a symmetry which leads to the continuum linearization having zero modes, eigenmodes and generalized eigenmodes corresponding to zero frequency. Viewed as a perturbation of the continuum system, the discrete, but "nearly" continuum problem is expected to have nearby modes to which these zero modes have been perturbed. If the coherent state is stable, these modes should be neutrally stable, *i.e.* that is, they must correspond to purely imaginary eigenvalues. (2) It is possible that discrete neutral modes may emerge from the continuous (phonon) spectrum.

Although some of these phenomena have been identified in the early numerical investigations [16], there has not been a systematic dynamical systems study relating particular resonances to the rate with which the kink is trapped by a "valley" in the PN potential or, once inside such a valley, the rate with which the kink relaxes to its asymptotic state. The main results in this direction date from the work of Ishimori and Munakata [27], in which the McLaughlin-Scott direct perturbation scheme [41] is used, valid in only in the nearly continuum regime, and the work of Boesch, Willis and El-Batanouny [8], which is based on numerical simulations and heuristic arguments.

In this paper, we introduce a systematic approach to the study of these phenomena.

The work is based on the recent work of one of us (MIW) with A. Soffer on a time dependent theory of metastable states in the context of: quantum resonances [51], ionization type problems (parametrically excited Hamiltonians) [52] and resonance and radiation damping of bound states in nonlinear wave equations [53]; see also [33, 42] A fruitful point of view adopted in these works and in the present work is that the dynamics can be understood as the interaction between a finite dimensional dynamical system, governing the bound state (internal modes plus kink) part of the solution and an infinite dimensional dynamical system and governing radiative behavior. Using the tools of scattering theory and the idea of normal forms, we derive a *dispersive normal form*, which is a closed (up to controllable error terms) finite dimensional system governing the internal mode components of the perturbation. From this normal form many aspects of the the large time asymptotic state are deducible.

The discrete systems we study (*e.g.* discrete sine-Gordon and discrete ϕ^4) depend on a discreteness parameter, d; as d increases the continuum limit is approached. The character of the normal form (topological character of its phase portrait) changes with d because the kinds of resonances which occur among discrete mode oscillations and continuum radiation (classifiable in terms of integer linear combinations of internal mode frequencies) change with d.

Our analytical and numerical studies lead us to the following picture concerning the dynamics in a neighborhood of the kink:
(1) The ground state kink, K_{gs}, is always Lyapunov stable [1]
(2) If d, the discretization parameter, is sufficiently large (approaching the spatial continuum case), the ground state kink is an attractor, i.e. is asymptotically stable. [2] *In this case the kink is approached at different algebraic rates depending on the range of d values. We infer this from the normal form analysis of section 4.*
(3) For d sufficiently small, our discrete nonlinear wave models have one or more branches of finite energy time-periodic solutions which bifurcate from K_{gs}; see Theorem 5.1 and Corollary 5.1. For the specific cases of discrete SG and discrete ϕ^4 our results imply, for various regimes of d, that there exist wobbling kinks, W. These are time periodic solutions with the same spatial symmetry as the kink and have been previously observed in numerical simulations. Additionally, our results imply in certain regimes of d, the existence of time periodic solutions (such as gW, eW in the ϕ^4 and gW in the SG), $u(t)$, with the property that $u(t) - K_{gs}$ is, to leading order in the direction of an even internal mode. Tables 3 and 7 in section 4 indicate the regimes in which these various solutions denoted occur. The wobbling solutions (W, gW, eW) may be viewed as a class of discrete breather / topological defect states. They are spatially localized

[1]If the initial data is in a small neighborhood of K_{gs}, then the solution remains in a small neighborhood of K_{gs} for all time. This notion of stability does not however imply convergence to K_{gs}.

[2]By asymptotic stability we mean that a small perturbation of the kink gives rise to a solution which converges as $t \to \pm\infty$, in some physically relevant norm, to a kink. Asymptotic stability is a notion of stability commonly associated with dissipative dynamical systems and is not commonly associated with general energy conserving systems. In this work we are studying infinite dimensional Hamiltonian systems on infinite spatial domains. These systems have the possibility of radiation of energy to infinity, while keeping the total energy of the system preserved. Thus dissipative behavior is realized through dispersion and eventual radiation of energy out of any compact set; see, for example, the short overview in [57] and references therein.

and time-periodic oscillations mounted on a static kink background. The usual discrete breathers [2, 38] are mounted on a zero background. This is analogous to the situation with solitons. Dark solitons of the defocusing nonlinear Schrödinger (NLS) equation are mounted on a non-zero continuous wave background, while standard solitons of focusing NLS sit on a zero background.
(4) Numerical simulations and the normal form analysis indicate that in various d regimes these time periodic states are local attractors for the dynamics.
(5) The analysis of section 5 implies some nonexistence results concerning solutions of discrete nonlinear wave equations in a neighborhood of the kink. We have that in certain regimes of the discreteness parameter, d, no nontrivial time-periodic solution exists, and that time quasiperiodic solutions do not exist in any regime of d. On the other hand, the normal form analysis and numerical simulations indicate, in some regimes of d, that periodic or quasiperiodic oscillations can be very long lived; see section 6, and in particular, the discussion of Regime VI in section 6.1. Thus, we may think of the system as possessing metastable periodic and quasi-periodic solutions. In regimes of d where we show that the wobbling kink, W, is unstable on long time scales due to a resonance of the "shape mode" with continuum radiation modes, we have the analogue of the the wobbling solution of continuum ϕ^4, proved to be stable on large but finite time scales by Segur [50]. On an infinite time scale this wobbling solution behaves as those of the discrete system for large enough d; eventually the oscillations damp at an algebraic rate leaving a kink in the limit [39, 49]. For the continuum system, the limiting kink may be traveling, while for the discrete system it is a static ground state (centered between lattice sites) kink.

In (2) the dispersive normal form has a dissipative character; the effect of coupling the internal mode oscillations to radiation is modeled by an appropriate nonlinear friction; see section 4 and the discussion in the introduction to [53] on another related model. The *damping* or *friction coefficients* are given by formulae which can be understood as a nonlinear generalization of *Fermi's golden rule*, arising in the context of the theory of spontaneous emission in atomic physics. Finally, it is worth noting that we obtain a dissipative and therefore apparently time-irreversible normal form from a system which is conservative and time-reversible. There is no contradiction because the dissipation is of an internal nature; it signifies the transfer of energy from the discrete internal mode oscillations to the continuum dispersive waves which propagate to infinity. That dissipative dynamical systems emerge from conservative systems which are a coupling of a low dimensional dynamics to infinite dimensional dynamics ("masses and springs coupled to strings") has been observed in many contexts; see, for example, [35, 5, 37] and the discussion in [51, 52, 53].

The paper is organized as follows:

- Section 2 begins with a general discussion of discrete nonlinear wave equations which support kink-like (heteroclinic) structures and then specializes to a discussion of the discrete sine-Gordon (SG) and discrete ϕ^4 systems.

- In section 3, we present the decomposition of solutions into discrete internal mode components and radiative components, enabling us to view the dynamics near a kink as the interaction of finite and infinite dimensional Hamiltonian systems.

- In section 4 the dispersive normal forms are derived and discussed for both discrete SG and discrete ϕ^4.
- In section 5, we prove that if Ω is an internal mode frequency and no multiple of it lies in the continuous spectrum of the kink (phonon band), then there is a family of finite energy time periodic solutions which bifurcate from the kink in the "direction" of the corresponding internal mode. The proof is based on the *Poincaré continuation* method and is an application of the implicit function theorem in an appropriate Banach space. This approach was used also by MacKay and Aubry [38], who constructed discrete breathers of nonlinear wave equations in the *anti-integrable* limit.
- In section 6 we combine the normal form analysis of section 4 and existence theory for periodic solutions of section 5 with observations based on numerical simulations to obtain a detailed picture of the dynamics in a neighborhood of the ground state kink.
- Finally, in section 7, we summarize our results and give directions of interest for future research.

1.1 Notation

- $\mathbb{Z}$ denotes the set of all integers and $\mathbb{R}$ denotes the set of real numbers.
- For $u = \{u_i\}_{i\in\mathbb{Z}}$, $\delta_h^2 u$ denotes the discrete Laplacian of u defined by:
$$(\delta_h^2 u)_i = h^{-2}\left(u_{i+1} - 2u_i + u_{i-1}\right). \tag{1.1}$$
In the case $h = 1$ we shall use the simplified notation $\delta^2 = \delta_1^2$.
- The inner product of vectors u and v in $l^2(\mathbb{Z})$ is given by
$$\langle u, v\rangle \; = \; \sum_j \bar{u}_j v_j. \tag{1.2}$$
- The t subscript denotes time partial derivatives, *e.g.* $u_t(t) = \partial_t u(t)$, whereas i denotes the lattice site numbering.
- $l^2(\mathbb{Z})$ is the Hilbert space of sequences $\{u_i\}_{i\in\mathbb{Z}}$ which are square summable.
- $H^s(I)$ denotes the Hilbert space of functions f, defined on $I \subset \mathbb{R}$ such that f and all its derivatives of order $\leq s$ are square-integrable. For the case of 2π periodic functions, $I = S^1_{2\pi}$, an equivalent norm on H^s is given by:
$$\|f\|^2_{H^s} = \sum_{n\in\mathbb{Z}} (1 + |n|^2)^s |f_n|^2, \tag{1.3}$$
where f_n denotes the n^{th} Fourier coefficient of f:
$$f_n = (2\pi)^{-\frac{1}{2}} \int_0^{2\pi} e^{-2\pi i n t} f(t)\ dt. \tag{1.4}$$

- For example, $H^2(\mathbb{R}; l^2(\mathbb{Z}))$ denotes the space of functions $f(t,i)$ which are H^2, as functions of t, with values in the space of $l^2(\mathbb{Z})$ functions.

- $\sigma(B)$ and $\sigma_{cont}(B)$ denote respectively the spectrum and the continuous (*phonon*) spectrum of the operator B.

- $0 < d$ denotes the *discretization parameter*; d large is the spatial continuum regime, while for d small the effects of discreteness are strong.

2 Discrete and continuum wave equations

2.1 General Background

Two model nonlinear wave equations on lattices that have played a central role in the theory of nonlinear waves are the *discrete sine-Gordon equation* (SG) and the *discrete ϕ^4 model* (ϕ^4). These equations may be viewed as governing the dynamics of a chain of unit mass particles which, in equilibrium, are equally spaced, a unit distance apart. The particles are then subjected to a conservative force derived from a potential. In terms of the displacement u_i of the i^{th} particle from equilibrium the equations of motion are[3]:

$$u_{i,tt} \ = \ (\delta^2 u)_i \ - \ d^{-2}V'(u_i). \tag{2.1}$$

The case of SG and ϕ^4 correspond, respectively, the choices of potential:

$$\begin{aligned} V(u) &= 1 - \cos u, \quad \text{(SG)} \\ V(u) &= \frac{1}{4}(1-u^2)^2. \quad (\phi^4) \end{aligned}$$

More generally, we assume V has three continuous derivatives and satisfies certain constraints appearing below, related to the existence of kink solutions or homoclinic orbits.

The parameter d is a fixed constant with, d^{-2}, having the interpretation of the ratio of on- site potential energy to elastic coupling energy.

Relation between discrete and continuum systems: The parameter d can also be seen to play the role of the reciprocal of the lattice spacing in passing between continuum and discrete models. Consider the continuum model governing the displacement $v(T,x)$:

$$v_{TT} = v_{xx} - V'(v). \tag{2.2}$$

Introducing the lattice spacing parameter, h, and replacing $u_{xx}(x)$ by $(\delta^2 u)_i$ we obtain the discrete nonlinear wave equation governing $v_i = v(T,i;h)$:

$$v_{i,TT} = (\delta_h^2 v)_i - V'(v_i). \tag{2.3}$$

The form of the discrete nonlinear wave equation we use is obtained by setting $t = h^{-1}T$ and defining the time-scaled displacement $u(t,i;h) = v(T,i;h)$. Then, $u(t,i;h)$ satisfies (2.1) with $d = h^{-1}$.

[3]We use the notational conventions introduced by Peyrard and Kruskal [48].

Taking the formal limit $d \uparrow \infty$ or equivalently $h \downarrow 0$ we have that

$$U(T,i) \equiv \lim_{d\to\infty} u(dT, i; d^{-1}) = \lim_{d\to\infty} v(T, i; d^{-1}) \tag{2.4}$$

satisfies the associated *continuum* nonlinear wave equation (2.2).
Hamiltonian structure: The discrete and continuum equations we consider are infinite dimensional Hamiltonian systems with Hamiltonian energy functionals[4]:

$$\mathcal{H} = \sum_i \frac{1}{2} u_{i,t}^2 + \frac{1}{2}\left(u_{i+1} - u_i\right)^2 + d^{-2} V(u_i) \tag{2.5}$$

in the discrete case and

$$\mathcal{H} = \int_{\mathbb{R}} \frac{1}{2}(u_T^2 + u_x^2) + V(u)\ dx. \tag{2.6}$$

Static kink solutions: Consider time-independent or *static* solutions of these dynamical systems. In each case, such solutions satisfy the equation obtained by setting time derivatives equal to zero. Thus, in the discrete case we have:

$$(\delta^2 K)_i = V'(K_i), \tag{2.7}$$

and in the continuum case

$$K''(x) = V'(K(x)) \tag{2.8}$$

Spatially uniform solutions occur at the critical points of the potential, V. Of particular interest are the static *kink* solutions. These are static solutions which are *heteroclinic.* That is, they are static solutions which can be viewed as connections, as $i \to \pm\infty$ (respectively $x \to \pm\infty$) in the phase space of two distinct "unstable" equilibria, values $K_*^{\pm}$ for which

$$\begin{aligned} V(K_*^+) &= V(K_*^-),\ V'(K_*^{\pm}) = 0 \\ V_*'' &\equiv V''(K_*^+) = V''(K_*^-) > 0. \end{aligned} \tag{2.9}$$

Kink solutions can also be constructed by variational methods. Consider the Hamiltonian energy functional, $\mathcal{H}$ restricted to t-independent functions:

$$h[u] = \sum_i \left(\frac{1}{2}(u_{i+1} - u_i)^2 + d^{-2} V(u_i) \right), \text{ discrete case} \tag{2.10}$$

$$h[u] = \int_{\mathbb{R}} \frac{1}{2} u_x^2 + V(u)\ dx \text{ continuum case.} \tag{2.11}$$

Then, the Euler Lagrange equations associated with $h[u]$ is the equation for the kink, (2.7). That is, if K_{gs} denotes a minimizer of $h[u]$ then since for all $\psi \in l^2(\mathbb{Z})$,

$$\frac{d}{d\tau}\ h[K_{gs} + \tau\psi]\ |_{\tau=0} = 0. \tag{2.12}$$

[4]There is freedom in the choice of potential V; we choose V so that the Hamiltonian energy of the static kink is finite.

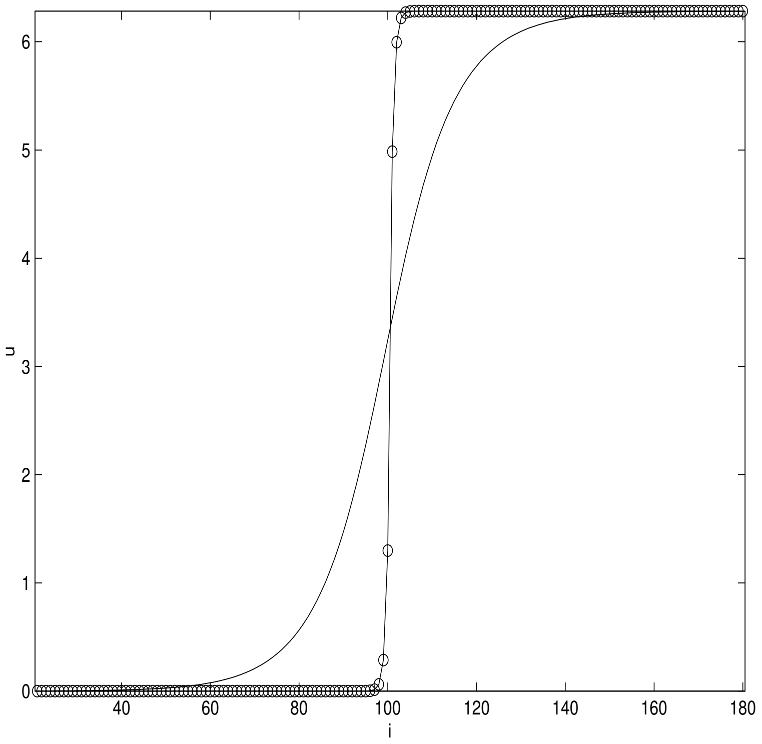

Figure 1: Ground state static kink for the very strongly discrete sine-Gordon model (–o–) $d = 0.6$, and very close to the continuum limit $d = 10$.

This implies that for all $\psi \in l^2(\mathbb{Z})$

$$\sum_i \left[-(\delta^2 K_{gs})_i + d^{-2} V'(K_{gs,i}) \right] \psi_i \;=\; 0. \tag{2.13}$$

This is equivalent to (2.7). A solution constructed by minimization of $h[u]$ is called a *ground state kink*.[5]

Invariance and broken invariance:

An important structural difference between the discrete and continuum cases is that the continuum case has greater symmetry. In particular, (2.2) has the property of translation and Lorentz invariance, while (2.1) does not. A consequence of this is that static solutions of (2.2) can be translated:

$$K(x) \mapsto K(x - x_0) \tag{2.14}$$

[5]A proof that the minimum of the functional (2.10) is attained can be given using the following strategy, used in a similar problem [56]: For positive integers, N, define $h_N[u]$ to be the truncated Hamiltonian, where the summation is taken over $-N \leq n \leq N$. Consider h_N, restricted to vectors satisfying $u_{\pm N} = K_*^{\pm}$. For any admissible vector, $u = \{u_i\}_{|i| \leq N}$, it is possible, by rearrangement, to replace it with another, v, which is monotonically increasing and for which $h[v] \leq h[u]$. Therefore the minimizer of $h_N[\cdot]$, $K_{gs}^{(N)}$, is monotonically increasing from K_*^- to K_*^+. Á priori estimates, derived from the Euler-Lagrange equation (2.7), and the boundary conditions enable one to pass to the limit and obtain a minimizer of $h[\cdot]$, $K_{gs} = \{K_{gs,i}\}_{i \in \mathbb{Z}}$, a monotonically increasing static kink.

to give a recentered kink and Lorentz boosted:

$$K(x) \mapsto K((x-vt)/\sqrt{1-v^2}),\ \ |v|<1, \tag{2.15}$$

to give a traveling solution of velocity v. These symmetries are absent in the discrete models. Discrete models do however have a discrete translation symmetry but in the models considered this does not give rise to discrete traveling waves.

Dynamic stability of kinks: The issue of dynamic stability is a subtle one. First, there is the question of what is the object we expect to be stable. Also, since our systems are infinite dimensional and not all norms are equivalent, different choices of norms will measure different phenomena. Here we briefly discuss three related notions of stability we have in mind: (a) orbital Lyapunov stability, (b) asymptotic stability and (c) linear spectral stability.

(a) *Orbital Lyapunov stability* means stability of the shape of the kink; if at $t=0$ the data is nearly shaped like a kink then it remains shaped like a kink for all $t \neq 0$. The kink-like part of the solution will typically move so the solution at different times is near some time-dependent spatial translate of the static kink (element of the symmetry group orbit of the static kink).

In the continuum case, orbital Lyapunov stability in the space $H^1(\mathbb{R})$ is a consequence of characterization of the kink as a local minimizer of $\mathcal{H}$. A detailed proof is presented in [24]. A simple proof of Lyapunov stability of ground state discrete kinks can be given based on the same ideas. [6]

(b) *Orbital asymptotic stability* means that if the initial data is nearly a kink then the solution converges to kink (possibly traveling, in the continuum case or pinned in the discrete case) as $t \to \infty$.

For both notions (a) and (b) we see that the stable object is the *family* of solitary wave solutions. That is, in the case where there is a multiparameter family of solutions (kinks, solitary waves ...), it is the collection of all such that is the stable object. Concerning the terminology *orbital stability*, this family of solutions is related to the set of functions generated by applying elements of the equation's symmetry group to the solution (here, static kink), and thus we can think of the group orbit as stable.

(c) *Spectral stability:*

As is well known, dynamic stability of the particular solution is related to the spectrum of the linearization of the dynamical system about this solution. Linearization about the kink gives an evolution equation for infinitesimal perturbations of the

[6] The proof is based on the following idea. Since K_{gs} is an energy minimizer, by (2.24), the second variation at the kink, B^2 is non-negative. In fact, it is strictly positive; that is, for all $\psi \in l^2(\mathbb{Z})$, $\langle \psi, B^2\psi\rangle \geq \omega_g^2\langle\psi,\psi\rangle$, where $\omega_g^2 = \omega_g^2(d) > 0$ is the discrete eigenvalue to which the zero mode of the continuum equation perturbs due to discretization of space. Suppose we have initial data near a kink: $u(0) = K_{gs} + v_0$, $\partial_t u(0) = v_1$ and let $u(t) = K_{gs} + v(t)$ be the resulting solution. Assume that $\|v_0, v_1\|_{l^2} \sim \varepsilon$, where ε is sufficiently small. Then, since K_{gs} is a critical point of $h[\cdot]$ we have:

$$\begin{aligned}\varepsilon \sim h[K_{gs}+v(t)]|_{t=0} - h[K_{gs}] &= h[K_{gs}+v(t)] - h[K_{gs}] = \frac{1}{2}\langle v(t), B^2 v(t)\rangle + \mathcal{O}(\|v(t)\|_{l^2}^3) \\ &\geq \frac{\omega_g^2}{2}\|v(t)\|_{l^2}^2 - c\|v(t)\|_{l^2}^3.\end{aligned}$$

implying that $\|v(t)\|_{l^2} \sim \mathcal{O}(\varepsilon)$ for all $t \neq 0$, and K_{gs} is stable.

following form:

$$\left(\partial_t^2 + B^2\right) p = 0. \tag{2.16}$$

For the discrete case:

$$B^2 p_i \;=\; -(\delta^2 p)_i \;+\; d^{-2} V''(K_i) p_i, \tag{2.17}$$

and for the continuum case:

$$B^2 p \;=\; -p_{xx} + V''(K(x))p. \tag{2.18}$$

At a minimum we expect that stability can hold only if no solutions of the linearized evolution equation, corresponding to finite energy initial conditions, can grow as $|t|$ increases. In carrying out linear stability analysis we seek solutions of the form $p_i = e^{\lambda t} P_i$ (respectively, $p = e^{\lambda t} P(x)$) and obtain linear eigenvalue problems of the form:

$$\left(B^2 + \lambda^2\right) P \;=\; 0. \tag{2.19}$$

Explicitly, we have:

$$\begin{aligned} -\lambda^2 P_i \;&=\; -(\delta^2 P)_i \;+\; d^{-2} V''(K_i) P_i, \text{ discrete case} \\ -\lambda^2 P \;&=\; -P_{xx} + V''(K(x))P. \text{ continuum case} \end{aligned}$$

We say λ *is in the l^2 spectrum (respectively, L^2 spectrum) of the linearization about the kink*, or simply *spectrum of the kink* if the operator $B^2 + \lambda^2$ does not have a bounded inverse on l^2 (respectively L^2). The spectrum will typically consist of two parts: (i) the point spectrum consisting of isolated eigenvalues of finite multiplicity, for which the corresponding solution of (2.19) is in the Hilbert space, and due to the infinite extent of the spatial domain (ii) continuous spectrum, whose corresponding solutions (*radiation or phonon modes*) of (2.19) are bounded and oscillatory over the entire spatial domain.

Note that the eigenvalue equation (2.19) has the following symmtery: if λ has the property that (2.19) has a nontrivial solution solution then $-\lambda, \bar{\lambda}$ and $-\bar{\lambda}$ also have this property. To avoid exponential growing solutions, we must require that the linearized spectrum is a subset of the imaginary axis. If this holds we say the solution is *spectrally stable.*

Spectrum of the kink:

We are interested in the set of λ's for which the eigenvalue equation

$$(B^2 + \lambda^2)P = 0 \tag{2.20}$$

has a nontrivial solution. We begin by discussing the spectrum of B^2 and then take square roots to a obtain the spectrum of the the linearization about the kink.

We now make two general remarks about the spectrum of the kink solution, one concerning the continuous spectrum and one concerning the point spectrum.

Continuous spectrum: The continuous spectrum is determined by the solutions of the constant coefficient equation obtained from (2.19) by evaluating its coefficients at spatial infinity. In the discrete case we obtain:

$$-\lambda^2 P_i \;=\; -(\delta^2 P)_i \;+\; d^{-2} V_*'' P_i, \tag{2.21}$$

where $V''_* = \lim_{i\to\pm\infty} V''(K_i)$. This constant coefficient equation can be solved in terms of exponentials which yield the character of the exact continuum eigensolutions of (2.19). We let $\lambda = i\omega$. We find bounded oscillatory solutions of the form: $P_n = \exp(\sqrt{-1}kn)$, $n \in \mathbb{Z}$, k real and arbitrary, where satisfies the dispersion relation:

$$\omega^2 = 4\sin^2(k/2) + d^{-2}V''_*. \tag{2.22}$$

It follows that the continuous spectrum of B^2 is the positive interval from $d^{-2}V''_*$ to $d^{-2}V''_* + 4$. Therefore, the continuous spectrum of the linearization about the kink solution consists of two intervals on the imaginary axis: $\pm i[d^{-1}\sqrt{V''_*}, \sqrt{4 + d^{-2}V''_*}]$.
Point spectrum: An important conclusion, concerning the point spectrum of kink for the continuum equation, can be made as a consequence of the equation's symmetry group. If $K(x)$ is a kink then translation invariance implies that $K'(x)$ is a zero mode, a solution of the linear eigenvalue problem with eigenvalue zero, $B^2K = 0$. This zero mode is often called the *Goldstone mode.* Since the eigenfunction, K' does not change sign, zero is the ground state energy (lowest point in the point spectrum) of the Sturm-Liouville operator $-\partial_x^2 + V''(K(x))$. This eigenvalue is of multiplicity one.

If one views the discrete model as a perturbation of the continuum model, due to the absence of corresponding symmetries in the discrete problem one expects the eigenvalue at zero to move, as d decreases from infinity (h, the lattice spacing, increases from zero), to the right of zero or to the left of zero. In terms of the spectrum of the kink (plus or minus the square root of the spectrum of B^2), this means that in the discrete case the spectrum of the kink consists of either (a) a purely imaginary pair, $\pm i\omega_s$ (stable case) or (b) a pair of real eigenvalues, symmetrically situated about the origin (unstable case). We shall see both cases in our study of specific discrete models and we shall refer to these eigenvalues and corresponding modes loosely as Goldstone modes as well.

As we shall see in the specific models considered, other eigenvalues may appear in the gap between the upper and lower branches of the continuous spectrum. Such modes of the linearization which lie in this gap are called *internal modes*, and their number and location can change with d. For SG we shall find that there are one or two pairs of internal modes, while for the ϕ^4 model there are two or three pairs of internal modes.

Finally, we remark that in the case of a *ground state kink*, one obtained by minimization of $h[u]$, the spectrum of B^2 is non-negative and the kink is spectrally stable. To see this, let K_{gs} denote a minimizer of $h[u]$, which as indicated above, is a critical point of $h[\cdot]$. Furthermore, for all $\psi \in l^2(\mathbb{Z})$,

$$\frac{d^2}{d\tau^2}\ h[K_{gs} + \tau\psi]\,|_{\tau=0} \geq 0. \tag{2.23}$$

A calculation yields that this is equivalent to:

$$\frac{1}{2}\langle\psi, B^2\psi\rangle\ \geq\ 0,\ \text{for all}\ \psi \in l^2(\mathbb{Z}). \tag{2.24}$$

Therefore, $d^2h[K_{gs}] = \frac{1}{2}B^2$, the second variation of $h[\cdot]$ at the ground state kink, is a nonnegative self-adjoint operator. It follows that the spectrum of the kink, $\pm i\sigma(B)$, lies on the imaginary axis.

2.2 The Sine-Gordon equation

Consider the discrete SG equation:

$$u_{i,tt} = (u_{i+1} + u_{i-1} - 2u_i) - \frac{1}{d^2}\sin u_i. \tag{2.25}$$

A static discrete 2π kink is a time-independent solution, $\{K_i\}_{i\in\mathbb{Z}}$ of (2.25) which satisfies the boundary conditions at infinity:

$$K_i \to 0, \text{ as } i \to -\infty, \text{ and } K_i \to 2\pi, \text{ as } i \to \infty \tag{2.26}$$

It is well-known that there are two static kink solutions, a high energy one centered on a lattice site and a low energy one centered between two consecutive lattice sites [48, 27, 15, 59, 54, 8, 9, 11, 7, 34, 30, 31]. The low energy kink corresponds to the minimizer of the static Hamiltonian energy, $h[u]$, displayed in (2.10). As d increases (the continuum limit) the energy difference between the two static kink solutions, the so-called Peierls-Nabarro (PN) barrier, tends to zero and the scaled limit $u(i; d^{-1}) = K_i$, with $i/d \equiv x$ fixed, converges to the continuum SG static kink solution

$$K_{SG}(x) = 4\tan^{-1}(e^x). \tag{2.27}$$

Linear stability analysis about the high energy and low energy kinks was carried out in [3]. From the general discussion of section 2.1, the dispersion relation defining the continuous (phonon) spectrum is $\omega^2 = d^{-2} + 4\sin^2(k/2)$. Therefore, B^2 has a band of continuous spectrum of length 4, $[d^{-2}, 4 + d^{-2}]$, and the continuous spectrum of the kink consists of the two bands, $\pm i[d^{-1}, \sqrt{4 + d^{-2}}]$.

For the case of the high energy kink, the point spectrum of B^2 contains a negative eigenvalue derived from the zero (Goldstone) mode associated with the continuum (translation invariant) case. Since the eigenvalue parameter in (2.19) is $-\lambda^2$, it follows that the spectrum of the high energy kink (parametrized by λ) consists of two discrete real (Goldstone) eigenvalues, one positive and one negative, $\pm\omega_{us}$. These occur at a distance of order $exp(-\pi^2 d)$ [27, 48, 4, 28].

The low energy kink, minimizes the Hamiltonian. The second variation of $h[u]$ at the kink, B^2, is therefore a self-adjoint and nonnegative operator. Its spectrum is therefore nonnegative and so the spectrum of the kink is purely imaginary. In this case, the Goldstone mode associated with translation invariance of the continuum problem gives rise to point spectrum consisting of a complex conjugate pair of eigenvalues with order of magnitude $\exp(-\pi^2 d)$. Furthermore, for $d > d_e$, $d_e \sim 0.515$ a spatially antisymmetric *edge mode* of energy ω_e^2 ($B^2 e = \omega_e^2 e$) appears whose corresponding energy has a distance from the phonon band edge of order $\mathcal{O}(d^{-4})$, for d large [34, 31]. This mode is not present in the continuum SG.

2.3 Discrete ϕ^4 Model

Consider the discrete ϕ^4 equation:

$$u_{i,tt} = (u_{i+1} + u_{i-1} - 2u_i) + \frac{1}{d^2}(u_i - u_i^3) \tag{2.28}$$

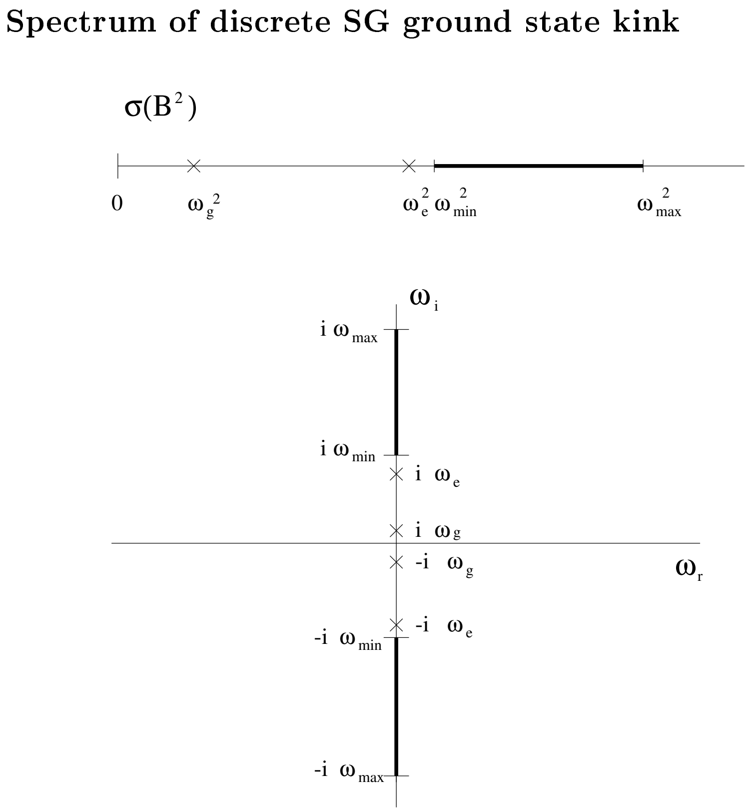

Figure 2: Upper panel: schematic of spectrum of B^2, $\sigma(B^2)$, consisting of two (for $d > d_e \sim 0.515$) positive discrete eigenvalues ($\omega_g^2 < \omega_e^2$) and a finite band of continuous spectrum extending from $\omega_{min}^2 = 1/d^2$ to $\omega_{max}^2 = \sqrt{4 + 1/d^2}$. Lower panel: schematic of spectrum of the kink, given by $\pm i\sigma(B)$.

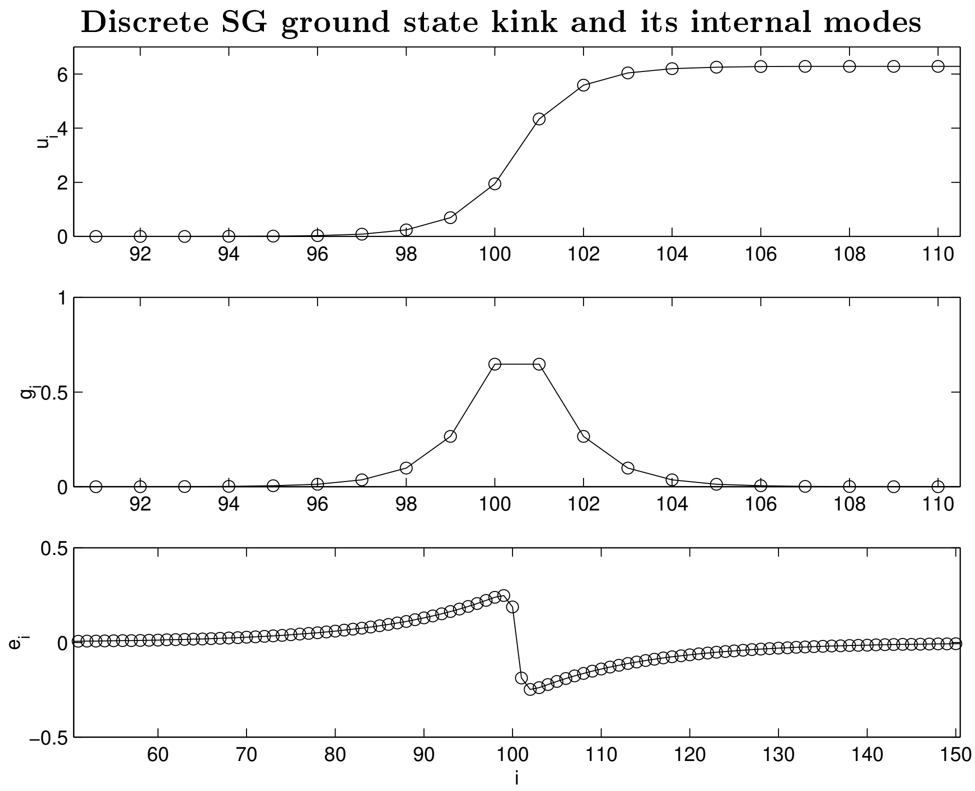

Figure 3: Three panels in order correspond to (a) discrete SG kink, (b) spatially even Goldstone mode (c) spatially odd edge mode (present for $d > d_e \sim 0.515$)

In most ways the situation is quite similar to that discussed for the discrete SG. The ϕ^4 model has low and high energy kinks. The low energy kink is centered between lattice sites while the high energy kink is centered at a lattice site. As d increases the energy difference, the PN barrier, tends to zero, and finally, in the scaled limit $u(i; d^{-1}) = K_i$, with $i/d \equiv x$ fixed, converges ot the continuum ϕ^4 kink,

$$K_{\phi^4}(x) \;=\; \tanh(x/\sqrt{2}). \tag{2.29}$$

Most qualitative properties of the spectrum of the linearization about the ϕ^4 kink are analogous to those in the SG case. The single key difference can be traced to the spectrum associated with the continuum case. In addition to the zero (Goldstone) mode, the spectrum of the operators B^2 has internal mode of odd parity with eigenfrequency $\omega_s^2 = 3/(4d^2)$. Therefore, the spectrum of the kink has purely imaginary internal modes associated with the energies $\omega_s = \pm i\sqrt{3}/(2d)$. These modes are called *shape modes.*

Turning now to the discrete ϕ^4 model we see that B^2 for the discrete case has the following properties:

- The dispersion relation is $\omega^2 = 2/d^2 + 4\sin^2(k/2)$, and therefore B^2 has continuous spectrum extending from $2/d^2$ to $2/d^2 + 4$.

- B^2 has a positive internal Goldstone mode with energy ω_g^2, so that $B^2 g = \omega_g^2 g$. This mode, which is traceable to the zero mode of the continuum model, is spatially even and ω_g is exponentially small in d [28].

- B^2 has an internal odd *shape mode* with energy ω_s^2, so that $B^2 s = \omega_s^2 s$. This mode, which is traceable to the internal shape mode of the continuum ϕ^4 model, is spatially odd.

- For $d > d_e$ ($d_e \sim 0.82$) B^2 has an internal *edge mode* which is even and with corresponding energy ω_e^2, with $B^2 e = \omega_e^2 e$, which emerges from the continuous spectrum. For large d we have [34, 31]

$$\omega_e{}^2 \sim 2d^{-2} - \frac{2}{15^2} d^{-6}. \tag{2.30}$$

It follows that the spectrum of the discrete ϕ^4 kink consists of pair of two or three complex conjugate pairs of internal modes at energies $\pm i\omega_g$, $\pm i\omega_s$, and for $d > d_e$, $\pm i\omega_e$.

In the next section we shall see that whether or not certain integer linear combinations of the internal mode frequencies land in the continuous spectrum determines the large time asymptotic behavior.

Spectrum of discrete ϕ^4 ground state kink

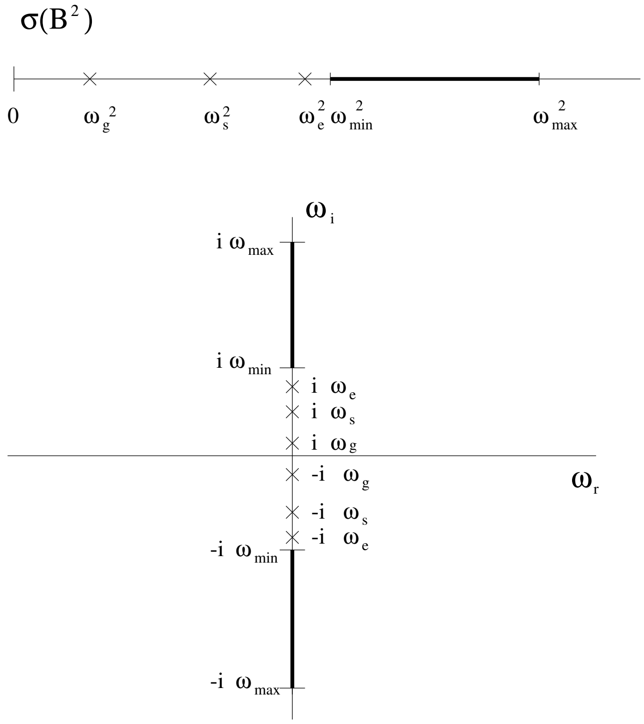

Figure 4: Upper panel: schematic of spectrum of B^2, $\sigma(B^2)$, consisting of three (for $d > d_e \sim 0.82$) positive discrete eigenvalues ($\omega_g^2 < \omega_s^2 < \omega_e^2$) and a finite band of continuous spectrum extending from $\omega_{min}^2 = 2/d^2$ to $\omega_{max}^2 = \sqrt{4 + 2/d^2}$. Lower panel: schematic of spectrum of the kink, given by $\pm i\sigma(B)$.

3 Resonances and radiation damping

That we can Lorentz boost a static kink and obtain a traveling kink on the spatial continuum (section 2) motivates the following question:

What happens if we attempt to cause a kink to propagate through the lattice?

The numerical and formal asymptotic investigation was initiated in [48],[47]. For example, choose as initial conditions for the discrete sine Gordon system the state $u_i(t = 0) = K(i/\sqrt{1 - v^2})$, where $K(x)$ is the continuum kink and $0 < |v| < 1$. Dispersive radiation plays an important role in the dynamics. The kink moves approximately as particle under the influence of the sinusoidal (Peierls-Nabarro) potential. As the kink propagates, its velocity alternately increases and decreases, depending on the location of its center of mass relative to the peaks and troughs of the potential. This oscillation leads to a resonance with the continuous spectrum [48, 8] and a transfer of energy from the propagating kink to radiation modes. Eventually, the kink has slowed so that its energy no longer exceeds the PN barrier and then executes a damped oscillation about a fixed lattice site to which it is pinned. It is this latter process that we study here.

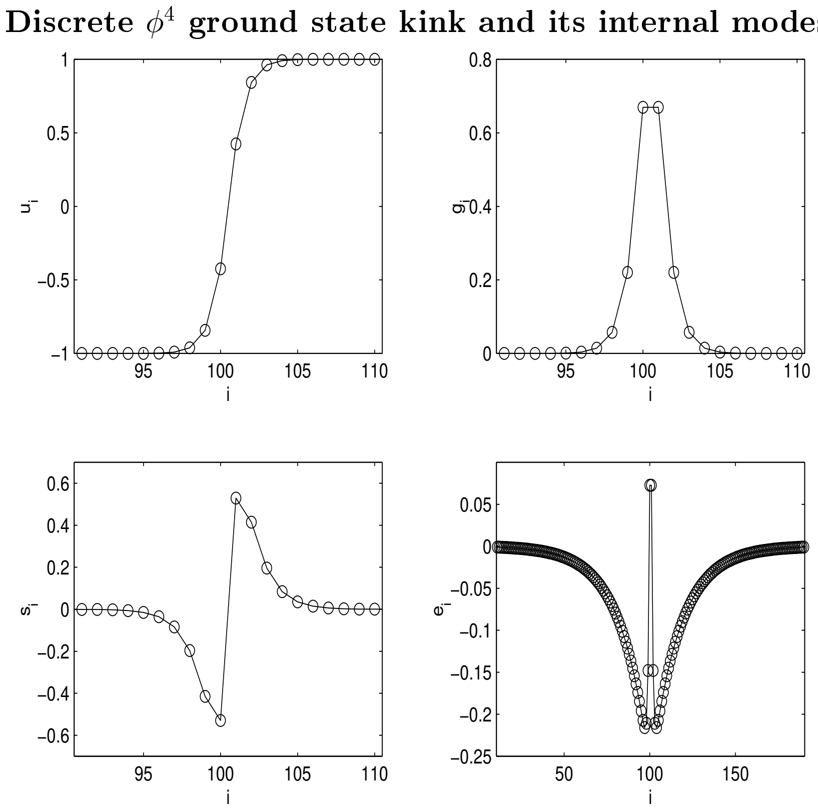

Figure 5: Top left panel as in figure one but for ϕ^4 and $d = 0.9$. Top right shows the g eigenfunction, bottom left the s_i and right the e_i.

The goal of this study is to, by analytic and numerical means,

- identify what the asymptotic state of the system is in different regimes of the discretization parameter d,
- find the rate of approach to this state.

We begin in the setting of the discrete ϕ^4 model, (2.28). This case is a more complicated than discrete SG; discrete ϕ^4 has either two or three internal modes, while discrete SG which has at most two. After a detailed treatment of the ϕ^4 case, we'll give an outline of the analogous results for SG.

We begin with a solution which is a small perturbation about a low energy (ground state) kink. This corresponds to solving the initial value problem for (2.28) with initial conditions:

$$u_i(0) = K_i + \varepsilon v_{0i}, \ \partial_t u_i(0) = \varepsilon v_{1i}, \tag{3.1}$$

where ε a small paramater. We then view the solution as

$$u_i(t) \ \equiv \ K_i \ + \varepsilon v_i(t), \tag{3.2}$$

where $v_i(t)$ denotes the perturbation about the kink. Equation (2.28) implies an evolution equation for v_i: $(\partial_t^2 + B^2)\, v \ = \ ...$ and since the data for v_i is small, it is natural to expand v_i in terms of the modes of the linearization about the kink. Recall that the operator B^2 is positive and self-adjoint, and has, depending on the range of $d's$ considered, two or three internal modes g, s, and e (if $d > d_e$):

$$\begin{aligned} &B^2 g_i = \omega_g^2 g_i,\ B^2 s_i = \omega_s^2 s_i,\ B^2 e_i = \omega_e^2 e_i \\ &0 < \omega_g^2 < \omega_s^2 < \omega_e^2 < 4 + 2d^{-2}, \end{aligned}$$

where

$$B^2 \psi_i \equiv -\delta^2 \psi_i + d^{-2}(3K_i^2 - 1)\psi_i. \tag{3.3}$$

We assume these internal modes to be normalized so that the set $\{g, s, e\}$ is orthonormal in $l^2(\mathbb{Z})$. We also introduce the operator which projects onto the orthogonal complement of the subspace of internal modes:

$$P_c \psi \equiv \psi - \langle g, \psi \rangle g - \langle s, \psi \rangle s - \langle e, \psi \rangle e \tag{3.4}$$

P_c is the projection onto the continuous spectral part of B^2 (phonon or radiation modes) and therefore the solutions of $(\partial_t^2 + B^2)u = 0$ with data in the range of P_c are expected to decay dispersively as $t \to \pm\infty$.

We expand the perturbation εv_i in terms of the internal mode subspace and its orthogonal complement and thus

$$u_i(t) = K_i + \varepsilon a(t) g_i + \varepsilon b(t) s_i + \varepsilon c(t) e_i + \varepsilon^2 \eta_i(t), \tag{3.5}$$

with

$$\begin{aligned} &\langle g, \eta(t) \rangle = \langle s, \eta(t) \rangle = \langle e, \eta(t) \rangle = 0, \\ &P_c \eta = \eta \end{aligned}$$

Substitution of (3.5) into (2.28) yields

$$\begin{aligned} & (a_{tt} + {\omega_g}^2 a) g_i + (b_{tt} + {\omega_s}^2 b) s_i + (c_{tt} + {\omega_e}^2 c) e_i + \varepsilon \partial_t^2 \eta_i \\ = & -\varepsilon B^2 \eta - d^{-2}(3\varepsilon K_i M_i^2 + \varepsilon^2 M_i^3 + 6\varepsilon^2 K_i \eta M_i + 3\varepsilon^3 M_i^2 \eta_i + \mathcal{O}(\varepsilon^4)) \end{aligned} \tag{3.6}$$

where:

$$M_i \equiv a(t) g_i + b(t) s_i + c(t) e_i. \tag{3.7}$$

Notice that from here on for simplicity and compactness we drop the spatial indices i.

We next project (3.6) onto the internal modes g, s and e, as well as on the range of P_c. This yields the following coupled system of four equations for the three internal mode amplitudes and the continuous spectral part:

$$\partial_t^2 a + {\omega_g}^2 a = -\frac{1}{d^2}\left(3\varepsilon\langle g, KM^2\rangle + \varepsilon^2\langle g, M^3\rangle + 6\varepsilon^2\langle g, KM\eta\rangle + 6\varepsilon^3\langle g, M^2\eta\rangle\right) + \mathcal{O}(\varepsilon^4) \tag{3.8}$$

$$\partial_t^2 b + {\omega_s}^2 b = -\frac{1}{d^2}\left(3\varepsilon\langle s, KM^2\rangle + \varepsilon^2\langle s, M^3\rangle + 6\varepsilon^2\langle s, KM\eta\rangle + 6\varepsilon^3\langle s, M^2\eta\rangle\right) + \mathcal{O}(\varepsilon^4) \tag{3.9}$$

$$\partial_t^2 c + {\omega_e}^2 c = -\frac{1}{d^2}\left(3\varepsilon\langle e, KM^2\rangle + \varepsilon^2\langle e, M^3\rangle + 6\varepsilon^2\langle e, KM\eta\rangle + 6\varepsilon^3\langle e, M^2\eta\rangle\right) + \mathcal{O}(\varepsilon^4)) \tag{3.10}$$

$$\partial_t^2 \eta + B^2 \eta = -\frac{1}{d^2} P_c\left(\varepsilon M^3 + 3KM^2 + \mathcal{O}(\varepsilon\eta M) + \mathcal{O}(\varepsilon^4\eta^3)\right). \tag{3.11}$$

The initial data for $a(t), b(t), c(t)$ is:

$$\begin{aligned}
a(0) &= \langle g, v_0\rangle,\ \partial_t a(0) = \langle g, v_1\rangle \\
b(0) &= \langle s, v_0\rangle,\ \partial_t b(0) = \langle s, v_1\rangle \\
c(0) &= \langle e, v_0\rangle,\ \partial_t b(0) = \langle e, v_1\rangle \\
\eta(0) &= P_c v_0,\quad \partial_t \eta(0) = P_c v_1
\end{aligned} \tag{3.12}$$

For simplicity we shall assume:

$$\eta(0) = 0,\ \partial_t \eta(0) = 0 \tag{3.13}$$

corresponding to perturbations of the kink which only excite the internal modes. The general case can be treated as well; see [53].

The system (3.8-3.11) may be viewed as finite dimensional Hamiltonian system governing three oscillators with amplitudes a, b and c and natural frequencies $\pm\omega_g, \pm\omega_s, \pm\omega_e$, coupled by nonlinearity to an infinite dimensional Hamiltonian wave equation for a field η. Systems of this type have been analyzed rigorously and the behavior of their solutions determined on short, intermediate and infinite time scales [52, 53]. The analysis we present uses and extends the methods of these works. Roughly speaking we transform the system (3.8)-(3.11) into an equivalent dynamical system, which is a perturbation of a *normal form* for which one obtains information on: (i) what the asymptotic state of the system is, and (ii) how this asymptotic state is approached.

4 The dispersive normal form

Our goal in this section is to derive the normal forms which give detailed information on the dynamics in a neighborhood of the ground state static kink of SG and ϕ^4. In particular, the normal forms anticipate the existence of time-periodic solutions. These predictions are upheld by the rigorous results of section 5. In section 6, the normal form analysis is then joined with the existence theory of section 5 and numerical simulations to fill out the picture of what the dynamics are in a neighborhood of the kink.

4.1 The normal form for discrete ϕ^4

At this stage, we have in (3.8-3.11) a formulation of the discrete ϕ^4 dynamical as a system governing the discrete internal modes interacting, due to nonlinearity, with a system governing dispersive waves (phonons). Our goal in this section is to present and implement a method, based on [52, 53], leading to a reformulation of the coupled discrete-continuum mode system (3.8-3.11) as a perturbed *dispersive normal form* in which the nature of the energy transfer among modes is made explicit.

Ideally, one could solve the equation for the dispersive part, η, explicitly in terms of the discrete mode amplitudes: a, b, and c and then substitute the result into the mode amplitude equations to get a closed system of equations for a, b, and c. This then could be used in the equation for η to determine its behavior. Due to the system's nonlinearity, one can't expect to solve for the exact behavior of η in terms of a, b and c. Instead we solve perturbatively in ε. Let

$$\eta \equiv \sum_{j=0}^{\infty} \varepsilon^j \eta^{(j)}. \tag{4.1}$$

Then,

$$\partial_t^2 \eta^{(0)} + B^2 \eta^{(0)} = -3d^{-2} K M^2. \tag{4.2}$$

The function η captures the leading order radiative response, to the internal mode excitations.

Note that $\eta^{(0)}$ is the solution of a forced wave equation. The forcing term in (4.2) involves M^2, which by (3.7), contains squares and cubes of a, b and c. Also, note that since the nonlinear coupling terms on the right hand sides of equations (3.8-3.10) are small, $a(t), b(t)$ and $c(t)$ are slow modulations of the exponentials $e^{\pm i\omega_g t}$, $e^{\pm i\omega_s t}$ and $e^{\pm i\omega_e t}$. The forcing on the right hand side of (4.2) will be resonant if nonlinearity, when acting on a, b and c, generates frequencies which lie in the spectrum of the operator B. Since B has a band of continuous spectrum, it can easily happen that integer linear combinations of the internal mode frequencies can lie in the continuous spectrum of B.

Figure 6 in section 4 displays the locations of the frequencies ω_g, ω_s and ω_e, their multiples and certain integer linear combinations relative to the continuous (phonon) spectrum. Figure 7 is the analogous plot for discrete SG.

The key calculation is to compute the effect of such resonances which result in the transfer of energy from the discrete to continuum modes.

Let

$$\begin{aligned} a(t) &= A(t)\exp(i\omega_g t) + \bar{A}(t)\exp(-i\omega_g t), \quad &(4.3)\\ b(t) &= B(t)\exp(i\omega_s t) + \bar{B}(t)\exp(-i\omega_s t), \quad &(4.4)\\ c(t) &= C(t)\exp(i\omega_e t) + \bar{C}(t)\exp(-i\omega_e t), \quad &(4.5) \end{aligned}$$

We further impose the constraints:

$$\begin{aligned} A_t\exp(i\omega_g t) + \bar{A}_t\exp(-i\omega_g t) &= 0\\ B_t\exp(i\omega_s t) + \bar{B}_t\exp(-i\omega_s t) &= 0\\ C_t\exp(i\omega_e t) + \bar{C}_t\exp(-i\omega_e t) &= 0. \end{aligned}$$

and obtain:

$$\begin{aligned} A_t &= (2i\omega_g)^{-1} e^{-i\omega_g t} F_1 \quad &(4.6)\\ B_t &= (2i\omega_s)^{-1} e^{-i\omega_s t} F_2 \quad &(4.7)\\ C_t &= (2i\omega_e)^{-1} e^{-i\omega_e t} F_3 \quad &(4.8) \end{aligned}$$

where $F_i = F_{i1} + F_{i2}$ (i=1,2,3). The 3×2 matrix F_{ij} is given by

$$F = -d^{-2} \begin{bmatrix} 3\varepsilon\langle g, KM^2\rangle + \varepsilon^2\langle g, M^3\rangle & 6\varepsilon^2\langle g, KM\eta\rangle + 3\varepsilon^3\langle g, M^2\eta\rangle \\ 3\varepsilon\langle s, KM^2\rangle + \varepsilon^2\langle s, M^3\rangle & 6\varepsilon^2\langle s, KM\eta\rangle + 3\varepsilon^3\langle s, M^2\eta\rangle \\ 3\varepsilon\langle e, KM^2\rangle + \varepsilon^2\langle e, M^3\rangle & 6\varepsilon^2\langle e, KM\eta\rangle + 3\varepsilon^3\langle e, M^2\eta\rangle \end{bmatrix} \tag{4.9}$$

We first solve (4.2) and obtain the expression for $\eta^{(0)}$ in terms of $a(t), b(t)$ and $c(t)$ or equivalently $A(t), B(t)$ and $C(t)$

$$\eta^{(0)} = -3d^{-2} \int_0^t \frac{\sin(B(t-\tau))}{B} \; P_c K M^2 d\tau \tag{4.10}$$

Recall that the dependence on the internal mode amplitudes is through M, defined in (3.7). Substitution of (4.10) into equations (4.6 -4.8) yields a closed system for the internal mode amplitudes through order ε^3. The key terms in this equation come from certain resonances and our goal now is to show how they arise.

The first column of terms in F involves the interactions among discrete modes. They do not generate frequencies contributing to any resonant forcing. The second column contains terms which couple the discrete bound state part to the continuum radiation modes. In order to identify all the resonances one has to explicitly expand out the F_{i2} terms and to use equation (4.10). We do not carry out the detailed computations in all detail here. Rather, we illustrate the key ideas and methodology by considering prototypical terms. A complete and rigorous implementation of these ideas in another nonlinear wave context is presented in [53].

We focus on the $\mathcal{O}(\varepsilon^2)$ term in F_{12} and *some* of its contributions to the equation for $A(t)$. In particular we shall consider all resonant contributions and a sample nonresonant contribution. By equation (4.6) we must then consider the expression:

$$3i\varepsilon^2 d^{-2} \omega_g^{-1} e^{-i\omega_g t} \langle Kg, M\eta^{(0)} \rangle. \tag{4.11}$$

Consider $\eta^{(0)}$.

$$\begin{aligned}
\eta^{(0)} &= -3d^{-2} \int_0^t \frac{\sin(B(t-\tau))}{B} \; P_c K M^2 d\tau \;=\; -\frac{3}{2iB} d^{-2} \int_0^t e^{iB(t-\tau)} \; P_c K M^2 d\tau \;+\; ... \\
&= \frac{3i}{2B} d^{-2} e^{iBt} \int_0^t e^{-iB\tau} \; P_c K g^2 a^2(\tau) d\tau \;+\; ... \\
&= \frac{3i}{2B} e^{iBt} \int_0^t e^{-iB\tau} \left(A^2(\tau) e^{2i\omega_g \tau} + 2|A(\tau)|^2 + \bar{A}^2(\tau) e^{-2i\omega_g \tau} \right) \; P_c K g^2 \; d\tau + ... \\
&= \frac{3i}{2B} e^{iBt} \int_0^t A^2(\tau) e^{-i(B-2\omega_g)\tau} \; P_c K g^2 d\tau + \frac{3i}{2B} e^{iBt} \int_0^t e^{-i(B+2\omega_g)\tau} \bar{A}^2(\tau) \; P_c K g^2 d\tau + ... \\
&\equiv \eta^{(0)}_{res} + \eta^{(0)}_{nr} + ...
\end{aligned} \tag{4.12}$$

We have only kept two terms in the above calculation: the only term leading to a resonant contribution in the A equation and one (of many) nonresonant terms.

We wish to expand $\eta^{(0)}$ using the following formula, which follows by straightforward integration by parts:

$$\begin{aligned}
& e^{iBt} \int_0^t e^{-i(B-\zeta)\tau} P_c \alpha(\tau) d\tau \\
=\; & ie^{iBt} (B-\zeta)^{-1} P_c e^{i\zeta t} \alpha(\tau) - ie^{iBt} (B-\zeta)^{-1} P_c \alpha(0) \\
& -ie^{iBt} \int_0^t e^{-i(B-\zeta)\tau} (B-\zeta)^{-1} P_c \; \partial_\tau \alpha(\tau) d\tau
\end{aligned} \tag{4.13}$$

with $\alpha(\tau) = A^2(\tau)\ P_c K g^2$, for example, and that τ-derivatives of A are of order ε. For the term $\eta^{(0)}_{res}$, $\zeta = 2\omega_g$, which for d in the range $[0.54, 0.6364]$ lies in the continuous spectrum; see Table 2 and Figure 6 below. Such resonant terms are of paramount interest and govern energy transfer. To treat these resonant terms, an appropriate modification of (4.13) is required. We use the following:
Let $\kappa = sgn(t)$, which is equal to $+1$ if $t > 0$ and -1 for $t < 0$.

$$
\begin{aligned}
& e^{iBt} \int_0^t e^{-i(B-\zeta)\tau} P_c\ \alpha(\tau) d\tau = \\
& ie^{iBt}(B - \zeta + i\kappa 0)^{-1} P_c\ e^{i\zeta t}\alpha(\tau) - ie^{iBt}(B - \zeta + i\kappa 0)^{-1} P_c\ \alpha(0) \\
& -ie^{iBt} \int_0^t e^{-i(B-\zeta)\tau}(B - \zeta + i\kappa 0)^{-1} P_c\ \partial_\tau \alpha(\tau) d\tau, \qquad (4.14)
\end{aligned}
$$

where

$$
(B - \zeta + i\kappa 0)^{-1} = \lim_{\epsilon \downarrow 0} (B - \zeta + i\kappa\epsilon)^{-1}. \qquad (4.15)
$$

Remark 4.1 *(1) The sense in which the operator expansions (4.13) and (4.14) are correct is in a distributional sense. That is, equality holds when multiplying both sides by a smooth function with spatial support which is compact and integrating both sides over all space.*
(2) Formula (4.14) is proved by first writing the integral on the left hand side as

$$
\int_0^t \exp(-i(B - \zeta + i\kappa\epsilon)\tau)\ P_c\alpha(\tau)\ d\tau. \qquad (4.16)
$$

For any $\epsilon > 0$ (4.13) can be used with ζ replaced by $\zeta - i\epsilon$. We then pass to the limit as $\epsilon \downarrow 0$.
(3) The choice of regularization, $+i0$ ($\kappa = 1$) for $t > 0$ and $-i0$ ($\kappa = -1$) for $t < 0$ is connected with the condition that the latter two terms in (4.14) consist of outgoing radiation at spatial infinity, and is therefore time-decaying in an appropriate local energy sense [53]. In this article, we take into account only the first term in (4.14). Reference [53] contains a fully detailed and rigorous treatment in a related context. Henceforth, we shall for simplicity assume $t > 0$ and therefore work with the $+i0$ regularization.
(4) If ζ does not lie in the continuous spectrum the formula (4.14) reduces to (4.13).

We now continue the expansion of $\eta^{(0)}$ using (4.13) to study $\eta^{(0)}_{nr}$ and (4.14) to study $\eta^{(0)}_{res}$:

$$
\begin{aligned}
\eta^{(0)}_{res} &= -\frac{3}{2} d^{-2} B^{-1} (B - 2\omega_g + i0)^{-1} A(t)^2\ P_c K g^2 + ... \\
\eta^{(0)}_{nr} &= -\frac{3}{2} d^{-2} B^{-1} (B + 2\omega_g)^{-1} \bar{A}(t)^2\ P_c K g^2 + ...
\end{aligned}
$$

Substitution of $\eta^{(0)} = \eta^{(0)}_{res} + \eta^{(0)}_{nr} + ...$ into (4.11) we have:

$$
\begin{aligned}
& 3i\varepsilon^2 d^{-2} \omega_g^{-1} e^{-i\omega_g t} \langle Kg, M\eta^{(0)} \rangle \\
& = 3i\varepsilon^2 d^{-2} \omega_g^{-1} e^{-i\omega_g t} \left(A e^{i\omega_g t} + \bar{A} e^{-i\omega_g t} \right) \langle Kg^2, \eta^{(0)} \rangle + ...
\end{aligned}
$$

$$= -\frac{9}{2} i\varepsilon^2 d^{-4} \omega_g^{-1} |A|^2 A \langle Kg^2, B^{-1}(B - 2\omega_g + i0)^{-1}\ P_c Kg^2 + ...\rangle$$
$$-\frac{9}{2} i\varepsilon^2 d^{-4} \omega_g^{-1} \bar{A}^3 e^{-3i\omega_g t} \langle Kg^2, B^{-1}(B + 2\omega_g)^{-1}\ P_c Kg^2\rangle + ...$$
$$\equiv \varepsilon^2 \left(-\Gamma_{2\omega_g} + i\Lambda_{2\omega_g}\right) |A(t)|^2 A(t) + \rho(t)\bar{A}^3(t) \tag{4.17}$$

To calculate Λ and Γ, we apply a generalization to self-adjoint operators of the well-known distributional identity:

$$\lim_{\epsilon\to 0} (\xi \pm i\epsilon)^{-1} = \text{P.V. } \xi^{-1} \mp i\pi\delta(\xi), \tag{4.18}$$

where $\delta(\xi)$ is the Dirac delta mass at $\xi = 0$ and P.V. denotes the principal value integral.

Therefore, using (4.18) we obtain:

$$\varepsilon^2 \Gamma_{2\omega_g} \equiv \varepsilon^2 \Gamma(2\omega_g) = \frac{9\pi}{4\omega_g^2} \varepsilon^2 d^{-4}\ \langle Kg^2, \delta(B - 2\omega_g) Kg^2\rangle, \tag{4.19}$$

$$\varepsilon^2 \Lambda_{2\omega_g} \equiv \varepsilon^2 \Lambda(2\omega_g) = -\frac{9}{2} \varepsilon^2 d^{-4} \langle Kg^2, P.V.(B - 2\omega_g) P_c Kg^2\rangle. \tag{4.20}$$

Remark 4.2 *(1) Had we done this calculation for the B (respectively, C) equation, we'd have obtained as a coefficient of $|B|^2 B$ (respectively, $|C|^2 C$) the quantity $\varepsilon^2(-\Gamma_{2\omega_s} + i\Lambda_{2\omega_s})$ (respectively, $\varepsilon^2(-\Gamma_{2\omega_e} + i\Lambda_{2\omega_e})$) (2) If $\zeta \in \sigma_{cont}(B)$, then Γ_ζ is always nonnegative and, generically, is strictly positive. It is the analogue of Fermi's golden rule wwhich arises in the context of the theory of spontaneous emission [36],[51]. Apart from a positive constant prefactor, Γ_ζ is the square of the Fourier transform of Kg^2 relative to the continuous spectral part of B evaluated at ζ.*

The above calculations yield the following information on the structure of the equation for $A(t)$:

$$A_t = \varepsilon^2 \left(-\Gamma_{2\omega_g} + i\Lambda_{2\omega_g}\right) |A|^2 A + ... \tag{4.21}$$

Extensive calculations, of which the above are representative, yield a system of the form:

$$\begin{aligned} A_t &= \varepsilon^2 \left(\alpha_1 |A|^2 + \alpha_2 |B|^2 + \alpha_3 |C|^2\right) A \\ &\quad \varepsilon^4 \left(\alpha_4 |A|^4 + \alpha_5 |A|^2 |B|^2 + \alpha_6 |B|^4 + \alpha_7 |B|^2 |C|^2 + \alpha_8 |C|^4\right) A \\ &+ \varepsilon \Xi_A(t, A, B, C; \varepsilon) \end{aligned}$$

$$\begin{aligned} B_t &= \varepsilon^2 \left(\beta_| A|^2 + \beta_2 |B|^2 + \beta_3 |C|^2\right) B \\ &\quad \varepsilon^4 \left(\beta_4 |A|^4 + \beta_5 |A|^2 |B|^2 + \beta_6 |B|^4 + \beta_7 |B|^2 |C|^2 + \beta_8 |C|^4\right) B \\ &+ \varepsilon \Xi_B(t, A, B, C; \varepsilon) \end{aligned}$$

$$
\begin{aligned}
C_t &= \varepsilon^2\left(\gamma_1|A|^2+\gamma_2|B|^2+\gamma_3|C|^2\right)C \\
&\quad \varepsilon^4\left(\gamma_4|A|^4+\gamma_5|A|^2|B|^2+\gamma_6|B|^4+\gamma_7|B|^2|C|^2+\gamma_8|C|^4\right)C \\
&+ \varepsilon\Xi_C(t,A,B,C;\varepsilon) \qquad (4.22)
\end{aligned}
$$

The coefficients α_j, β_j and γ_j are, in general, complex numbers. The terms Ξ_A, Ξ_A and Ξ_A involve bounded and oscillatory complex exponentials in t multiplying monomials in A, B, C of cubic or higher degree. Also, in order to obtain the fifth degree terms it is necessary to construct η through second order in ε (and therefore the continuous spectral part of the perturbation about the kink, $\varepsilon^2\eta$, through ε^4. Coupling to η is neglected as is the dynamical equation for η. The preceding calculation gives $\alpha_1 = -\Gamma_g + i\Lambda_g$ plus a further term contributed by the $\mathcal{O}(\varepsilon^2)$ entry of F_{11} in (4.9). An exhaustive tabulation of all coefficients $\alpha_j, \beta_j, \gamma_j$ would be, to put it midly, a very lengthy exercise. Since the principal effect we seek to illuminate is that of nonlinear resonant coupling on the internal mode amplitudes $|A|, |B|$ and $|C|$, we only tabulate those coefficients up to the order considered which may play a role.

For this it is convenient to introduce the notation:

$$G(\zeta) = P_c B^{-1}(B-\zeta+i0)^{-1}P_c \qquad (4.23)$$

Table 1A: Principal ϕ^4 g-mode coefficients

Term	Coefficient (α_j)
$\|A\|^2A$	$-\frac{9}{2}id^{-4}\omega_g^{-1}\langle Kg^2, G(2\omega_g)Kg^2\rangle$
$\|B\|^2A$	$-9id^{-4}\omega_g^{-1}\langle Kgs, G(\omega_g+\omega_s)Kgs\rangle$
$\|C\|^2A$	$-9id^{-4}\omega_g^{-1}\langle Kge, G(\omega_g+\omega_e)Kge\rangle$
$\|A\|^4A$	$-\frac{3}{4}id^{-4}\omega_g^{-1}\langle g^3, G(3\omega_g)g^3\rangle$
$\|B\|^4A$	$-\frac{9}{4}id^{-4}\omega_g^{-1}\langle gs^2, G(\omega_g+2\omega_s)gs^2\rangle$
$\|C\|^4A$	$-\frac{9}{4}id^{-4}\omega_g^{-1}\langle ge^2, G(\omega_g+2\omega_e)ge^2\rangle$
$\|A\|^2\|B\|^2A$	$-\frac{9}{2}id^{-4}\omega_g^{-1}\langle g^2s, G(2\omega_g+\omega_s)g^2s\rangle$
$\|A\|^2\|C\|^2A$	$-\frac{9}{2}id^{-4}\omega_g^{-1}\langle g^2e, G(2\omega_g+\omega_e)g^2e\rangle$
$\|B\|^2\|C\|^2A$	$-9id^{-4}\omega_g^{-1}\langle gse, G(\omega_g+\omega_s+\omega_e)gse\rangle$

Table 1B: Principal ϕ^4 s-mode coefficients

Term	Coefficient (β_j)
$\|B\|^2B$	$-\frac{9}{2}id^{-4}\omega_s^{-1}\langle Ks^2, G(2\omega_s)Ks^2\rangle$
$\|A\|^2B$	$-9id^{-4}\omega_s^{-1}\langle Kgs, G(\omega_g+\omega_s)Kgs\rangle$
$\|C\|^2B$	$-9id^{-4}\omega_s^{-1}\langle Kse, G(\omega_s+\omega_e)Kse\rangle$
$\|B\|^4B$	$-\frac{3}{4}id^{-4}\omega_s^{-1}\langle s^3, G(3\omega_s)s^3\rangle$
$\|A\|^4B$	$-\frac{9}{4}id^{-4}\omega_s^{-1}\langle sg^2, G(2\omega_g+\omega_s)sg^2\rangle$
$\|C\|^4B$	$-\frac{9}{4}id^{-4}\omega_s^{-1}\langle se^2, G(\omega_s+2\omega_e)se^2\rangle$
$\|A\|^2\|B\|^2B$	$-\frac{9}{2}id^{-4}\omega_s^{-1}\langle gs^2, G(\omega_g+2\omega_s)s^2g\rangle$
$\|A\|^2\|B\|^2B$	$-\frac{9}{2}id^{-4}\omega_s^{-1}\langle gs^2, G(2\omega_s-\omega_g)s^2g\rangle$
$\|B\|^2\|C\|^2B$	$-\frac{9}{2}id^{-4}\omega_s^{-1}\langle s^2e, G(2\omega_s+\omega_e)s^2e\rangle$
$\|A\|^2\|C\|^2B$	$-9id^{-4}\omega_s^{-1}\langle gse, G(\omega_s+\omega_e-\omega_g)gse\rangle$
$\|A\|^2\|C\|^2B$	$-9id^{-4}\omega_s^{-1}\langle gse, G(\omega_g+\omega_s+\omega_e)gse\rangle$

Table 1C: Principal ϕ^4 e-mode coefficients

Term	Coefficient (γ_j)
$\lvert C\rvert^2C$	$-\frac{9}{2}id^{-4}\omega_e^{-1}\langle Ke^2, G(2\omega_e)Ke^2\rangle$
$\lvert B\rvert^2C$	$-9id^{-4}\omega_e^{-1}\langle Kse, G(\omega_s+\omega_e)Kse\rangle$
$\lvert A\rvert^2C$	$-9id^{-4}\omega_e^{-1}\langle Kge, G(\omega_g+\omega_e)Kge\rangle$
$\lvert C\rvert^4C$	$-\frac{3}{4}id^{-4}\omega_e^{-1}\langle e^3, G(3\omega_e)e^3\rangle$
$\lvert B\rvert^4C$	$-\frac{9}{4}id^{-4}\omega_e^{-1}\langle s^2e, G(2\omega_s+\omega_e)s^2e\rangle$
$\lvert A\rvert^4C$	$-\frac{9}{4}id^{-4}\omega_e^{-1}\langle g^2e, G(2\omega_g+\omega_e)g^2e\rangle$
$\lvert C\rvert^2\lvert B\rvert^2C$	$-\frac{9}{2}id^{-4}\omega_e^{-1}\langle se^2, G(\omega_s+2\omega_e)se^2\rangle$
$\lvert C\rvert^2\lvert B\rvert^2C$	$-\frac{9}{2}id^{-4}\omega_e^{-1}\langle se^2, G(2\omega_e-\omega_s)se^2\rangle$
$\lvert C\rvert^2\lvert A\rvert^2C$	$-\frac{9}{2}id^{-4}\omega_e^{-1}\langle ge^2, G(\omega_g+2\omega_e)ge^2\rangle$
$\lvert C\rvert^2\lvert A\rvert^2C$	$-\frac{9}{2}id^{-4}\omega_e^{-1}\langle ge^2, G(2\omega_e-\omega_g)ge^2\rangle$
$\lvert B\rvert^2\lvert A\rvert^2C$	$-9id^{-4}\omega_e^{-1}\langle gse, G(\omega_g+\omega_s+\omega_e)gse\rangle$
$\lvert B\rvert^2\lvert A\rvert^2C$	$-9id^{-4}\omega_e^{-1}\langle gse, G(\omega_s+\omega_e-\omega_g)gse\rangle$

Before discussing the information contained in these tables, we note that the system (4.22) can be further simplified. Using a near-identity transformation:

$$\left(\tilde{A},\tilde{B},\tilde{C}\right) = (A,B,C) + \mathcal{O}\left(|A|^2+|B|^2+|C|^2\right) \tag{4.24}$$

the system (4.22) can be transformed into a new system for $\tilde{A},\tilde{B}$ and $\tilde{C}$ of a very similar form, but with the following modifications:

- The real parts of the coefficients are the same but the imaginary parts may be modified.
- The $\varepsilon^2\Xi$ terms are now replaced by terms of order ε^6

We refer to the system governing $\tilde{A}$, $\tilde{B}$ and $\tilde{C}$, obtained in the manner, after neglecting the Ξ terms, as a *dispersive normal form.*

While complicated in its details, there is a simple way to think about this normal form. We introduce the *internal mode powers* [7]:

$$P = |\tilde{A}|^2,\ \ Q = |\tilde{B}|^2,\ \ R \equiv |\tilde{C}|^2. \tag{4.25}$$

The equations for the powers are:

$$\begin{aligned} P_t &= 2\varepsilon^2\left(\alpha_1^rP+\alpha_2^rQ+\alpha_3^rR\right)P \\ &\quad +2\varepsilon^4\left(\alpha_4^rP^2+\alpha_5^rPQ+\alpha_6^rQ^2+\alpha_7^rQR+\alpha_8^rR^2\right)P \qquad (4.26)\\ Q_t &= 2\varepsilon^2\left(\beta_1^rP+\beta_2^rQ+\beta_3^rR\right)Q \\ &\quad +2\varepsilon^4\left(\beta_4^rP^2+\beta_5^rPQ+\beta_6^rQ^2+\beta_7^rQR+\beta_8^rR^2\right)Q \qquad (4.27)\\ R_t &= 2\varepsilon^2\left(\gamma_1^rP+\gamma_2^rQ+\gamma_3^rR\right)R \\ &\quad +2\varepsilon^4\left(\gamma_4^rP^2+\gamma_5^rPQ+\gamma_6^rQ^2+\gamma_7^rQR+\gamma_8^rR^2\right)R, \qquad (4.28) \end{aligned}$$

where α_j^r, β_j^r and γ_j^r denote the real parts of the coefficients α_j^r, β_j^r and γ_j^r appearing in (4.22). The real parts do not change under the near identity change of variables:

[7] Strictly speaking, by (4.24) P, Q and R are only approximately equal, respectively, to the Goldstone, shape and edge mode powers.

$A \mapsto \tilde{A}, B \mapsto \tilde{B}, C \mapsto \tilde{C}$, and are therefore given by the real parts of the coefficients displayed in Table 1. In general, as the reader may note, a contribution to the above mentioned internal mode power equations of the form $|A|^{2m_1}|B|^{2m_2}|C|^{2m_3}$ comes from a frequency combination $m_1\omega_g+m_2\omega_s+m_3\omega_e$ landing in the band of continuous spectrum through a term

$$(M(K,g,s,e), G(m_1\omega_g + m_2\omega_s + m_3\omega_e)M(K,g,s,e)) \tag{4.29}$$

where M is the appropriate monomial combination of the relevant spatial parts.

As the discreteness parameter, d, varies the spectrum of the kink (the continuous spectrum and the number and location of the internal modes) changes. As indicated in Figure 6, for different values of d various integer linear combinations of the internal mode frequencies, the simplest of which are those appearing as arguments of $G(\cdot)$ in Table 1, may lie in the continuous spectrum.

How does this influence the character of the normal form?

Let ζ denote one such linear combination of frequencies. By (4.18):

$$\begin{aligned} G(\zeta) &= P_c\ B^{-1}(B-\zeta)^{-1}\ P_c, \quad \zeta \notin \sigma_{cont}(B) \\ G(\zeta) &= P_c\ \text{P.V.}\ B^{-1}(B-\zeta)^{-1}\ P_c\ - i\frac{\pi}{\zeta}P_c\ \delta(B-\zeta)\ P_c, \quad \zeta \in\ \sigma_{cont}(B). \end{aligned} \tag{4.30}$$

Each of the coefficients of the system listed in Table 1 is a positive multiple of an expression of the form $-i\langle f, G(\zeta)f\rangle$, where f is spatially localized. Therefore, if ζ does not lie in the continuous spectrum of B, the associated coefficient of the system for the powers P, Q, R, $\alpha^r = \Re\alpha, \beta^r = \Re\beta$ or $\gamma^r = \Re\gamma$, will be zero. On the other hand, if ζ **does** lie in the continuous spectrum of B, this coefficient will be of the form:

$$\begin{aligned} \Gamma_\zeta &\equiv -\frac{\pi}{\zeta}\langle P_c f, \delta(B-\zeta)\ P_c f\rangle \\ &= -\frac{\pi}{\zeta}\left|\mathcal{F}_B[f](\zeta)\right|^2, \end{aligned}$$

where $\mathcal{F}_B$ denotes the Fourier transform with respect to the continuous spectral part of the operator B. Generically, one has Γ_ζ is strictly negative. Therefore, such resonances are associated with nonlinear damping of energy in the internal modes. This does not contradict the Hamiltonian character of the equations of motion. The $\tilde{A}, \tilde{B}, \tilde{C}$ system is coupled to the dispersive system governing η; damping of the discrete mode amplitudes implies a transfer of energy from the discrete to continuum modes. The information contained in Figure 6 enables us to determine, for each d, which combinations of harmonics appear in the phonon band. Then Tables 1A, 1B and 1C, together with (4.26-4.28) give us the precise form of the internal mode power equations, from which we can ascertain the detailed behavior of solutions in a neighborhood of the static kink.

In the Table 2 (below) we present the form of the internal mode power equations for different ranges of the parameter, d. There are numerous changes in the form of these equations as d varies, so for clarity, we indicate only the key transitions. These key transitions occur across values of d where there is a topological change in the phase portrait of the system governing the internal mode powers. Such changes are found

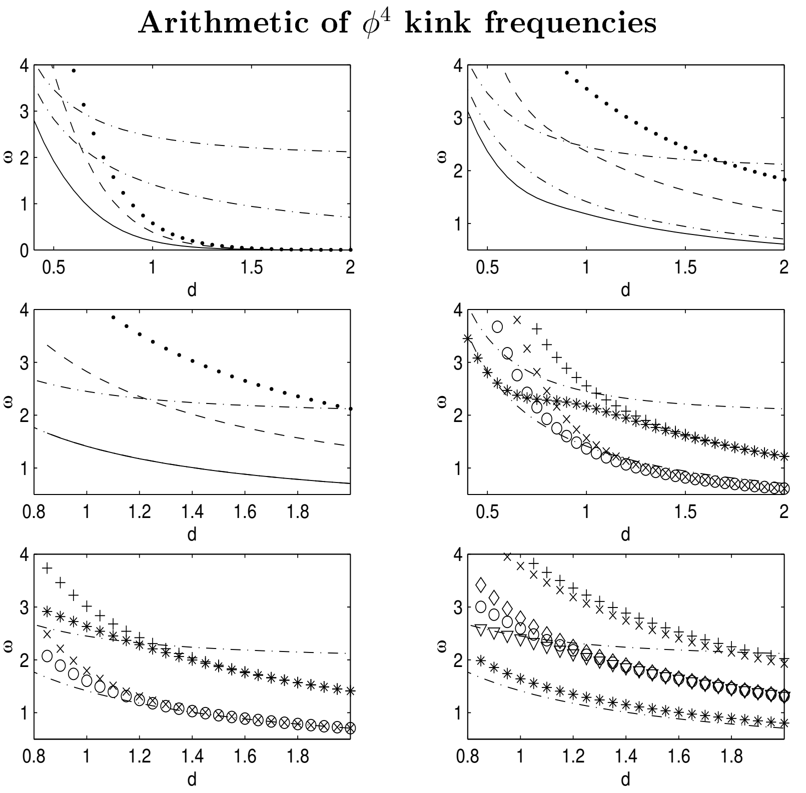

Figure 6: Integer linear combinations of internal mode frequencies: In all 6 panels, the band is indicated by dash-dotted lines. Top left shows the goldstone frequency as a function of d (solid) and its second (dashed) and third (dotted) harmonics for ϕ^4. The top right panel follows the same sequence of symbols for the shape mode harmonics while the left panel of the second row does so for the edge mode. The right panel of the second row shows the combinations of ω_g, ω_s that can appear in the band. In particular: $\omega_g + \omega_s$:o, $2\omega_g + \omega_s$:x, $2\omega_s + \omega_g$: $+$, $2\omega_s - \omega_g$: $*$. Similarly in the bottom left panel for the g, e modes. In particular: $\omega_g + \omega_e : o, 2\omega_g + \omega_e : x, 2\omega_e + \omega_g : +, 2\omega_i - \omega_g : *$. And in the case of bottom right panel s, e modes are shown but so are combinations of all 3 frequencies. In particular: $\omega_s+\omega_e : o, 2\omega_s+\omega_e : x, 2\omega_e+\omega_s : +, 2\omega_i-\omega_s : *, \omega_s+\omega_g+\omega_e :$ diamonds, $\omega_s + \omega_e - \omega_g$:down triangles.

due to a change in the nature of the set of equilibria, *e.g.* going from a system with one line of equilibria to one where there are two lines of equilibria, or due to a change in the number of internal modes (jump in the dimensionality of the phase portrait). The latter transition occurs at $d = d_e,\ d_e \sim 0.82$, when a point eigenvalue emerges from the edge of the continuous spectrum and appears as a third internal mode, e, an *edge mode*, with corresponding frequency ω_e.

Table 2: ϕ^4 internal mode power equations

Regimes of d	Resonances	System Form
$I: d < 0.5398$	$\{2\omega_s - \omega_g, \ldots\}$	$P_t = 0,\ Q_t = -\varepsilon^4\{PQ^2\}$
$II:\ 0.5398 \le d < 0.6145$ $2\omega_g \in \sigma_{cont}$	$2\omega_g,\ \omega_g + \omega_s$ $2\omega_s - \omega_g$	$P_t = -\varepsilon^2 P\{P,Q\}$, $Q_t = -\varepsilon^2 PQ\{1, \varepsilon^2\{Q\}\}$
$III:\ 0.6145 \le d < 0.6364$	$2\omega_g,\ 2\omega_s - \omega_g$	$P_t = -\varepsilon^2\{P^2\}$, $Q_t = -\varepsilon^4\{PQ^2\}$
$IV:\ 0.6364 \le d < 0.6679$ $2\omega_g \notin \sigma_{cont}$	$\omega_g + \omega_s$ $2\omega_s - \omega_g$	$P_t = -\varepsilon^2\{PQ\}$, $Q_t = -\varepsilon^2\{PQ\{1, \varepsilon^2\{Q\}\}\}$
$V:\ 0.6679 \le d < d_e$ $d_e \sim 0.82$	$\{3\omega_g, 4\omega_g, 2\omega_s - \omega_g\}$ $\{\omega_g + \omega_s,\ 2\omega_g + \omega_s\}$	$P_t = -\varepsilon^4 P^3\{1, \varepsilon^2 P\} - \varepsilon^2 PQ\{1, \varepsilon^2 P\}$, $Q_t = -\varepsilon^2 PQ\{1, \varepsilon^2\{P, Q\}\}$
$VI:\ d_e \le d < 0.9229$ ω_e appears	$\{4\omega_g, 5\omega_g, 2\omega_s - \omega_g\}$ $\omega_g + \omega_s, 2\omega_g + \omega_s, 2\omega_e - \omega_s$ $\omega_g + \omega_e, 2\omega_g + \omega_e, \omega_e + \omega_s - \omega_g$	$P_t = -\varepsilon^2 P\{Q\{1, \varepsilon^2 P\}, R\{1, \varepsilon^2 P\}, \varepsilon^4 P^3\} + ...$ $Q_t = -\varepsilon^2 PQ\{1, \varepsilon^2\{P, Q, R\}\} + ...$ $R_t = \varepsilon^2 PR\{1, \varepsilon^2\{P, Q\}\} - \varepsilon^4 QR^2 + ...$
$VII:\ 0.9229 \le d < d_*$ $d_* \sim 1.2234$ $2\omega_s \in \sigma_{cont}$	$\{n\omega_g\}_{5 \le n \le 38}, 2\omega_s$ $\omega_g + \omega_s, \omega_g + \omega_e, 2\omega_g + \omega_s$, $2\omega_g + \omega_e, 2\omega_g + 2\omega_s, \omega_g + 2\omega_s$, $\omega_g + \omega_s + \omega_e, \omega_s + \omega_e, 2\omega_e - \omega_s$ $2\omega_e - \omega_g, \omega_e + \omega_s - \omega_g, 2\omega_s - \omega_g$	$P_t = -\varepsilon^{2n-2}\{P^n\} + ...$ $Q_t = -\{\varepsilon^2 Q^2\} + ...$ $R_t = -\varepsilon^2 R\{Q, P\} + ...$
$VIII:\ d_* \le d$ $2\omega_e \in \sigma_{cont}$	$n\omega_g\ (5 \le n \le N), 2\omega_s, 2\omega_e$	$P_t = -\varepsilon^{2n-2}\{P^n\} + ...$ $Q_t = -\{\varepsilon^2 Q^2\} + ...$ $R_t = -\{\varepsilon^2 R^2\} + ...$

Remark on notation: We illustrate the notation of the table with the following example. Consider the regime V. This regime can be broken into three subregimes illustrated in the following table:

Table 3: internal mode power equations for subregime V

Subregime of d	Resonances	System Form
$a)\ 0.6679 \le d < 0.743$	$3\omega_g, \omega_g + \omega_s$ $2\omega_s - \omega_g$	$P_t = -\varepsilon^2 C_1 PQ - \varepsilon^4 C_2 P^3$, $Q_t = -\varepsilon^2 C_3 PQ - \varepsilon^4 C_4 PQ^2$
$b)\ 0.743 \le d < 0.7622$	$3\omega_g, 4\omega_g$ $\omega_g + \omega_s, 2\omega_s - \omega_g$	$P_t = -\varepsilon^2 C_1 PQ - \varepsilon^4 C_2 P^3 - \varepsilon^6 C_5 P^4$, $Q_t = -\varepsilon^2 C_3 PQ - \varepsilon^4 C_4 PQ^2$
$c)\ 0.7622 \le d < 0.7687$	$3\omega_g, \omega_g + \omega_s, 2\omega_s - \omega_g$ $4\omega_g, 2\omega_g + \omega_s$	$P_t = -\varepsilon^2 C_1 PQ - \varepsilon^4 C_2 P^3 - \varepsilon^4 C_6 P^2 Q - \varepsilon^6 C_5 P^4$ $Q_t = -\varepsilon^2 C_3 PQ - \varepsilon^4 C_4 PQ^2 - \varepsilon^4 C_7 P^2 Q$
$c)\ 0.7687 \le d < d_e$ $d_e \sim 0.82$	$\omega_g + \omega_s, 2\omega_g + \omega_s$ $4\omega_g, 2\omega_s - \omega_g$	$P_t = -\varepsilon^2 C_1 PQ - \varepsilon^4 C_6 P^2 Q - \varepsilon^6 C_5 P^4$ $Q_t = -\varepsilon^2 C_3 PQ - \varepsilon^4 C_4 PQ^2 - \varepsilon^4 C_7 P^2 Q$

Although the details of the system form change between regimes, the topological character of the phase portrait and therefore the qualitative nature of the solutions does not change; each phase portrait has $P = 0$ as a stable line of equilibria. For regime

III, Table 2 is read as follows: in this regime some or all resonances occur from among each of the indicated sets: $\{3\omega_g, 4\omega_g\}$, and $\{\omega_g + \omega_s, 2\omega_s - \omega_g, 2\omega_g + \omega_s\}$, giving rise to terms in the following manner:

$$k\omega_g + l\omega_s + m\omega_e \ \rightarrow \ \varepsilon^{2n-2} P^{|k|} Q^{|l|} R^{|m|}, \quad k, l, m \in \mathbb{Z}, \quad |k| + |l| + |m| = n. \tag{4.31}$$

Thus the sets in curly brackets in Table 2 are to be viewed as columns of a "menu" from which one (or the dynamical system) chooses all or some items (resonant combinations) depending on the subregime of d. For a given subregime, this choice of subset gives rise to linear combination with *nonnegative coefficients*, C_j, of the corresponding monomials in P, Q and R in the power equations. Therefore $P_t, Q_t, R_t \leq 0$. Generically , we have $C_j > 0$.

It is straightforward to analyze the sets of equilibria and their stability for each of the systems in Table 2. These take the form of constant vectors with *at most* one nonzero component. These states are dynamically stable. If we take the view that the system of power equations determines the nonlinear dynamics near the static kink we anticipate that:

- the zero solution of the internal mode power equations corresponds to the ground state static kink solution discrete nonlinear equation. We denote the ground state kink by K_{gs}.

- a nonzero equilibrium state with $Q \neq 0$ corresponds to a time periodic solution:

  $$u_i \sim K_{gs,i} + \cos(\omega_s t) s_i. \tag{4.32}$$

  We call such a periodic solution of the full nonlinear dynamical system, which would have the same symmetry as the kink, a *wobbling kink*, which we designate by sW or simply W.

- a nonzero equilibrium state with $P \neq 0$ power equations corresponds to a time periodic solution:

  $$u_i \sim K_{gs,i} + \cos(\omega_g t) g_i. \tag{4.33}$$

  We call such a periodic solution a *g-wobbling kink*. We denote this state by gW.

- a nonzero equilibrium state with $R \neq 0$ power equations corresponds to a time periodic solution:

  $$u_i \sim K_{gs,i} + \cos(\omega_e t) g_i. \tag{4.34}$$

  Such a periodic solution of the full nonlinear dynamical system, would not have the same symmetry as the kink. We call such a periodic solution an *e-wobbling kink*. We denote this state by eW.

Below, we present a table of the kinds of static and periodic states anticipated by the normal form / internal mode power equation analysis.

Table 4: ϕ^4 normal form equilibria and anticipated coherent structures

Regime of d	Equilibria	Coherent structures
I: $d < 0.5398$	$\{(P,0) : P \geq 0\}$ $\{(0,Q) : Q \geq 0\}$	$K_{gs},\ W, gW$
II-III: $0.5398 \leq d < 0.6364$	$\{(0,Q) : Q \geq 0\}$	$K_{gs},\ W$
IV: $0.6364 \leq d < 0.6679$	$\{(0,Q) : Q \geq 0\}$ $\{(P,0) : P \geq 0\}$	$K_{gs},\ W,\ gW$
V: $0.6679 \leq d < d_e$ $d_e \sim 0.82$	$\{(0,Q) : Q \geq 0\}$	$K_{gs},\ W$
VI: $d_e \leq d < 0.9229$	$\{(0,Q,0) : Q \geq 0\}$ $\{(0,0,R) : R \geq 0\}$	$K_{gs},\ W,\ eW$
VII: $0.9229 \leq d < 1.2234$ $d_* \sim 1.2234$	$\{(0,0,R) : R \geq 0\}$	$K_{gs},\ eW$
VIII: $d_* \leq d$	$\{(0,0,0)\}$	K_{gs}

4.2 The normal form for discrete sine-Gordon

The procedure for deriving the normal form for the internal mode amplitudes and the internal mode power equations presented in sections 3 and 4.1 can be applied to the discrete sine-Gordon equation as well. The implementation is actually simpler because for discrete SG there are only two internal modes: g and e; see section 2. Therefore, the decomposition of the solution is:

$$u_i(t) = K_i + \varepsilon a(t) g_i + \varepsilon b(t) e_i + \varepsilon^2 \eta_i(t), \tag{4.35}$$

where

$$\begin{aligned} &\langle g, \eta(t)\rangle = \langle e, \eta(t)\rangle = 0 \\ &P_c \eta \equiv \eta - \langle g, \eta(t)\rangle g - \langle e, \eta(t)\rangle e \ = \ \eta(t) \end{aligned}$$

As in the previous subsection the amplitude equations for the slowly varying modulation functions can be obtained:

$$\begin{aligned} A_t &= \varepsilon^2 \left(\alpha_1 |A|^2 + \alpha_2 |B|^2\right) A + \varepsilon^4 \alpha_3 |B|^4 A + \Xi_A(A,B,t) \\ B_t &= \varepsilon^2 \left(\beta_1 |A|^2 + \beta_2 |B|^2\right) A + \varepsilon^4 \beta_3 |B|^4 A + \Xi_B(A,B,t) \end{aligned} \tag{4.36}$$

The coefficients α_j, β_j can be evaluated along the lines detailed in the pervious section and are tabulated below.

Table 5A : Principal SG g-mode coefficients

$\lvert A\rvert^2 A$	$-\frac{1}{8} d^{-4} {\omega_g}^{-1} \langle \sin K g^2, G(2\omega_g) \sin K g^2 \rangle$
$\lvert A\rvert^4 A$	$-\frac{3}{4(3!)^2} d^{-4} \omega_g^{-1} \langle \cos K g^3, G(3\omega_g) \cos K g^3 \rangle$
$\lvert B\rvert^2 A$	$-\frac{1}{2} d^{-4} \omega_g^{-1} \langle \sin K ge, G(\omega_g + \omega_e) \sin K ge \rangle$
$\lvert B\rvert^4 A$	$-\frac{9}{4(3!)^2} d^{-4} {\omega_g}^{-1} \langle \cos K ge^2, G(\omega_g + 2\omega_e) \cos K ge^2 \rangle$
$\lvert A\rvert^2 \lvert B\rvert^2 A$	$-\frac{18}{4(3!)^2} d^{-4} \omega_g^{-1} \langle \cos K g^2 e, G(2\omega_g + \omega_e) \cos K g^2 e >$

Table 5B : Principal SG e-mode coefficients

$\|B\|^2B$	$-\frac{1}{8}d^{-4}\omega_e^{-1}\langle\sin Ke^2, G(\omega_e)\sin Ke^2\rangle$
$\|B\|^4B$	$-\frac{3}{4(3!)^2}d^{-4}\omega_e^{-1}\langle\cos Ke^3, G(3\omega_e)\cos Ke^3\rangle$
$\|A\|^2B$	$-\frac{1}{2}d^{-4}\omega_e^{-1}\langle\sin Kge, G(\omega_g+\omega_e)\sin Kge\rangle$
$\|A\|^4B$	$-\frac{9}{4(3!)^2}d^{-4}\omega_e^{-1}\langle\cos Keg^2, G(\omega_e+2\omega_g)\cos Keg^2\rangle$
$\|A\|^2\|B\|^2B$	$-\frac{18}{4(3!)^2}d^{-4}\omega_e^{-1}\langle\cos Ke^2g, G(\omega_g+2\omega_e)\cos Ke^2g\rangle$
$\|A\|^2\|B\|^2B$	$-\frac{18}{4(3!)^2}d^{-4}\omega_e^{-1}\langle\cos Ke^2g, G(2\omega_e-\omega_g)\cos Ke^2g\rangle$

As with discrete ϕ^4, the details of the internal mode power equations change as d varies due to the different types of resonances with the continuous spectrum which may occur. For discrete SG there are essentially only two regimes, and one value of the parameter d across which there is a topological change in the phase portraits. Since the detailed picture is simpler we tabulate it in greater detail.

Figure 7 displays the variation of the internal mode frequencies (ω_g, ω_e), certain multiples of them and certain other integer linear combinations of them. As with discrete ϕ^4, transitions in the structure of the normal form occur across values of d for which there is a change in the set of integer linear combinations which lie in the band of continuous spectrum. The precise normal form and power equations can be worked out using the coefficient Table 5 and the expression for $G(\zeta)$, (4.30). Notice that only the leading order terms are given in these internal mode power equations.

Table 6: SG internal mode power equations

Regime of d	Resonances	System Form
I: $d < d_e \sim 0.515$	None	$P_t = 0$
II: $d_e \leq d < .565$	$2\omega_e - \omega_g, \{3\omega_g - \omega_e\}$	$P_t = -\varepsilon^6\{P^3Q\},\ Q_t = -\varepsilon^4\{PQ^2\}$
III: $0.565 \leq d < 0.65$	$2\omega_g, 2\omega_e - \omega_g$	$P_t = -\varepsilon^2\{P^2\}, Q_t = -\varepsilon^4\{PQ^2\}$
$0.65 \leq d < 0.7$	$2\omega_g, \omega_g + \omega_e$	$P_t = -\varepsilon^2P\{P, Q\}$, $Q_t = -\varepsilon^2PQ\{1, \varepsilon^2Q\}$
$0.7 \leq d < 0.76$	$2\omega_g, 3\omega_g, \omega_g + \omega_e$, $2\omega_e - \omega_g$	$P_t = -\varepsilon^2P\{P, Q, \varepsilon^4P^2\}$, $Q_t = -\varepsilon^2PQ\{1, \varepsilon^2Q\}$
$0.76 \leq d < 0.785$	$3\omega_g, \omega_g + \omega_e$, $2\omega_e - \omega_g$	$P_t = -\varepsilon^2P\{Q\} - \varepsilon^2\{P^2\}$, $Q_t = -\varepsilon^2PQ\{1, \varepsilon^2Q\}$
$0.785 \leq d < 0.8$	$3\omega_g, 4\omega_g$ $\omega_g + \omega_e, 2\omega_e - \omega_g$	$P_t = -\varepsilon^2P\{Q, \varepsilon^2P^2, \varepsilon^6P^4\}$, $Q_t = -\varepsilon^2PQ\{1, \varepsilon^2PQ\}$
$0.8 \leq d < 0.847$	$3\omega_g, 4\omega_g, 2\omega_e - \omega_g$ $\omega_g + \omega_e, 2\omega_g + \omega_e$	$P_t = -\varepsilon^2P\{Q, \varepsilon^2P^2, \varepsilon^2PQ, \varepsilon^4P^3\}$, $Q_t = -\varepsilon^2PQ\{1, \varepsilon^2Q, \varepsilon^2P\}$
$0.847 \leq d < d_*$ $d_* \sim 0.86$	$3\omega_g, 4\omega_g, 5\omega_g, 2\omega_e - \omega_g$ $\omega_g + \omega_e, 2\omega_g + \omega_e$	$P_t = -\varepsilon^2P\{Q, \varepsilon^2P^2, \varepsilon^4P^3, \varepsilon^2PQ, \varepsilon^6P^4\}$, $Q_t = -\varepsilon^2PQ\{1, \varepsilon^2Q, \varepsilon^2P\}$
IV: $d_* \leq d < 0.9$	$3\omega_g, 4\omega_g, 5\omega_g, 2\omega_e$ $\omega_g + \omega_e, 2\omega_g + \omega_e, 2\omega_e - \omega_g$	$P_t = -\varepsilon^2P\{Q, \varepsilon^2P^2, \varepsilon^4P^3, \varepsilon^2PQ\}$, $Q_t = -\varepsilon^2Q\{P, Q, \varepsilon^2PQ, \varepsilon^2P^2\}$
$0.9 \leq d < 0.99$	$4\omega_g, 5\omega_g, 2\omega_e$ $\omega_g + \omega_e, 2\omega_g + \omega_e, 2\omega_e - \omega_g$	$P_t = -\varepsilon^2P\{Q, \varepsilon^4P^3, \varepsilon^2PQ, \varepsilon^4P^4\}$, $Q_t = -\varepsilon^2Q\{P, Q, \varepsilon^2PQ, \varepsilon^2P^2\}$
$0.99 \leq d < 1.003$	$5\omega_g, 2\omega_e, 2\omega_e - \omega_g$ $\omega_g + \omega_e, 2\omega_g + \omega_e$	$P_t = -\varepsilon^2P\{Q, \varepsilon^2PQ, \varepsilon^6P^4\}$, $Q_t = -\varepsilon^2Q\{Q, \varepsilon^2PQ, \varepsilon^2P^2\}$
$1.003 \leq d$	$n\omega_g\ (n \geq 5), 2\omega_e, \omega_g + \omega_e$ $2\omega_g + \omega_e, \omega_g + 2\omega_e$	$P_t = -\varepsilon^2P\{Q, \varepsilon^2PQ, \varepsilon^{2n-2}P^{n-1}, \varepsilon^2Q^2, ...\}$, $Q_t = -\varepsilon^2Q\{P, Q, \varepsilon^4P^2, \varepsilon^4PQ, ...\}$

The inferred coherent structures are displayed in the following table.

Table 7: SG normal form equilibria and anticipated coherent structures

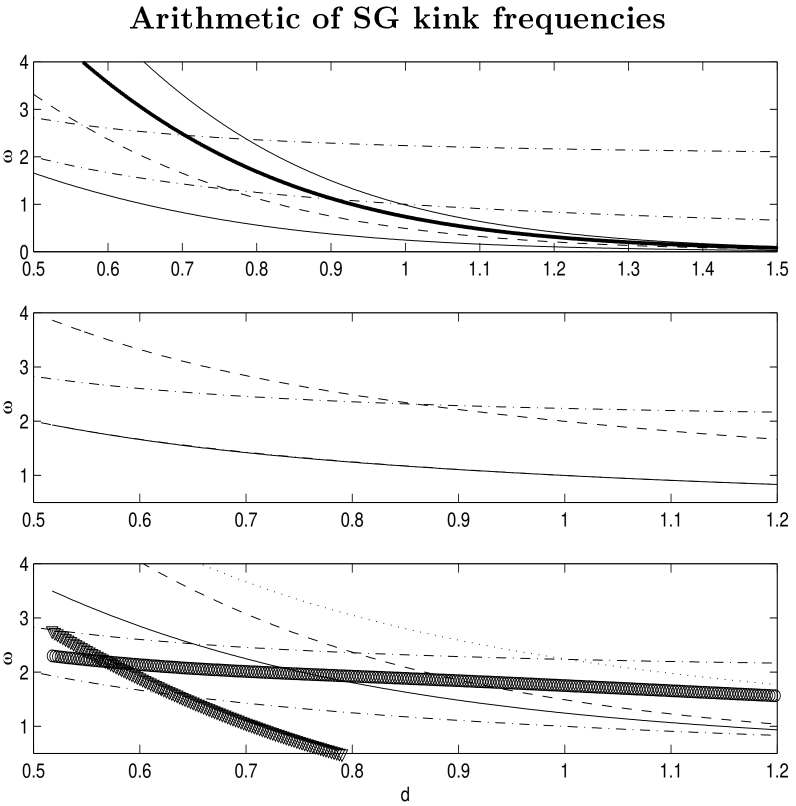

Figure 7: Top panel shows the Goldstone harmonics (solid: first, dashed: second, thick:third and again solid: fourth). Higher harmonics of g will also be relevant, but are not shown here. Middle panel shows the shape mode (solid line) that lives close to the band edge (maximum bifurcation is of the order of 0.01) and its second harmonic (dashed). Finally, lower panel shows mixed combinations of harmonics (solid: to $\omega_g + \omega_s$, dashed: $2\omega_g + \omega_e$ and dotted to $\omega_g + 2\omega_e$). The circles denote $2\omega_e - \omega_g$ while the down triangles $3\omega_g - \omega_e$ -see note below-. In all cases the phonon band edges are shown by dash-dot lines.

Regime of d	Equilibria	Coherent structures
I: $d < d_e$	$P \geq 0$	$K_{gs},\ gW$
II: $d_e \leq d < 0.565$	$\{(P,0),(0,Q) : P \geq 0,\ Q \geq 0\}$	$K_{gs},\ W,\ gW$
III: $0.565 \leq d < d_*$ $d_* \sim 0.86$	$\{(0,Q) : Q \geq 0\}$	$K_{gs},\ W$
IV: $d_* \leq d$	$\{(0,0)\}$	K_{gs}

5 Time periodic solutions

5.1 Existence of wobbling kinks

From the discussion of the previous section, we expect that the dispersive normal form we have derived for discrete nonlinear wave equations (in particular, discrete

SG and ϕ^4) models the dynamics in a neighborhood of the static kink solution. This normal form captures the effects of nonlinear resonant interactions of the internal and continuum mode fluctuations about the kink. Tables 4 and 7 indicate for discrete ϕ^4 discrete SG the anticipated existence of periodic solutions which bifurcate from the static kink solution. In this section we prove, under suitable nonresonance hypotheses, the existence of such time periodic solutions.

In tables 3 and 5 we see that these normal forms fall into two categories (i) those for which the origin is the only equilibrium (d sufficiently large, $d > d_*$) (ii) d is such that the normal form admits one or two lines of equilibria. In case (i) we see that the zero solution is asymptotically stable. By (3.5) and (4.35) this suggests that the ground state kink is a stable attractor. At d_* there is a bifurcation in the phase portrait; for $d < d_*$, zero is no longer an isolated equilibrium. Rather, the normal form now has a line of stable equilibria passing through the origin. This then suggests an approximate solution of the nonlinear wave equation of the form:

$$u_j \sim K_j \ + \ \varepsilon B_{eq} \cos(\Omega t) \xi_{\Omega,j}, \quad j \in \mathbb{Z} \tag{5.1}$$

where ξ_Ω denotes an internal mode Ω its corresponding frequency; $B\chi_\Omega = \Omega\chi_\Omega$ and ε is small. If such a family of periodic solutions exists, we say this family bifurcates from the kink solution in the direction of the internal mode, ξ_Ω. Such directions for bifurcation are available for $d < d_*$.

For $d < d_*$ are there bifurcating time periodic solutions?

In view of the analysis of the regime $d > d_*$, one must be cautious about reaching a conclusion about the large time behavior on the basis of the above approximation. In fact we learn from the regime $d > d_*$ that radiation damping, due to resonant coupling of oscillations to the continuum, may lead to the slow decay of a solution which appears to be time-periodic on shorter time scales.

On the other hand, given the approximate periodic solution (5.1) it is certainly natural to attempt a perturbative (in ϵ) construction of a true time-periodic solution. The approach we use is the Poincaré continuation, which is standard in the persistence theory of periodic solutions of systems of ordinary differential equations [14]. As in typical perturbation expansions, one expects a hierarchy of linear inhomogeneous problems governing contributions to the expansion at various orders in ϵ. Solvability at each order requires that one can arrange for the solution to each inhomogeneous problem to be time periodic of some common period. That this can be achieved in the problem at hand follows from the following nonresonance condition, verified in our numerical investigation of the spectrum of the kink:

(NR) *Assume that no integer multiple of the internal mode frequency Ω lies in the continuous spectrum of B.*

A precise statement of the result is as follows:

Theorem 5.1 *Let $K = \{K_i\}_{i\in\mathbb{Z}}$ denote a ground state kink. Assume that the linear operator, B, acting on the space $l^2(\mathbb{Z})$, has a simple eigenvalue, Ω, with corresponding eigenfunction, ξ_Ω satisfying $B\xi_\Omega = \Omega\xi_\Omega$. Also assume the nonresonance condition* **(NR)**. *Then, in a neighborhood of K, there is a curve of solutions $\epsilon \mapsto y(t;\epsilon)$ passing through the ground state kink with the following properties:*

- *There is a number* $\epsilon_0 > 0$ *such that* $y(t;\epsilon)$ *is defined for all* $\epsilon < \epsilon_0$.
- $y(t;0) = K$
- $y(t;\epsilon)$ *has period* $2\pi/\omega(\epsilon)$ *in* t, *where* $\omega^2(\epsilon) = \Omega^2(1+\mathcal{O}(\epsilon))$ *is a smooth function with* $\omega(0) = \Omega$.
- $y(t;\epsilon) \in l^2(\mathbb{Z})$
- $y_i(t;\epsilon) = K_i + \epsilon\cos(\omega(\epsilon)t)\xi_{\Omega,i} + \mathcal{O}(\epsilon^2)$.

The next result, a simple consequence of the proof of Theorem 5.1, yields the class of solutions which we call *wobbling kinks.*

Corollary 5.1 *For discrete SG, the periodic solution bifurcating from the kink in the direction of the spatially odd edge mode* ($Be = \omega_e e$) *has the same symmetry as the SG kink around its center. For discrete* ϕ^4 *the periodic solution bifurcating from the kink in the direction of the spatially odd shape mode* ($Bs = \omega_s s$) *has the same symmetry as the* ϕ^4 *kink.*

We seek a solution in the form:

$$u_i = K_i + b(t)\xi_{\Omega,i} + \eta_i,\ \ i \in \mathbb{Z}. \tag{5.2}$$

Substitution of (5.2) into (2.28) and then projection of the resulting equation separately onto the eigenvector ξ_Ω and its orthogonal complement yields the coupled system for the shape mode amplitude and the radiation components [8]

$$\partial_t^2 b + \Omega^2 b = -d^{-2}\langle \xi_\Omega, \mathcal{V}[b\xi_\Omega + \eta](b\xi_\Omega + \eta)^2\rangle \tag{5.4}$$
$$\partial_t^2 \eta + B^2 \eta = -d^{-2} P_c \mathcal{V}[b\xi_\Omega + \eta](b\xi_\Omega + \eta)^2, \tag{5.5}$$

where

$$\mathcal{V}[M] = \int_0^1 (1-\theta)V'''(K+\theta M)d\theta. \tag{5.6}$$

Remark 5.1 *It is possible to formulate the proof of Theorem 5.1, as essentially a consequence results in [14] (Chapter 14, Theorem 2.1), applied to (5.4-5.5); a simple generalization of the result to an infinite dimensional setting is required. In this context, hypothesis* **(NR)**, *corresponds to the hypothesis that* 1 *be a simple Floquet multiplier of the unperturbed linear problem obtained by setting the right hand sides of (5.4-5.5) equal to zero. In this paper we present a direct proof of Theorem 5.1 in order to make our study elementary and self-contained.*

[8] Here we employ the Taylor expansion for the function $W = V'$:

$$W(K+M) = W(K) + W'(K)M + \int_0^1 (1-\theta)W''(K+\theta M)d\theta M^2 \tag{5.3}$$

We shall be considering *small* perturbations of the static kink, and therefore introduce rescaled internal mode and radiation components:

$$b = \epsilon b_1, \quad \eta = \epsilon \eta_1, \tag{5.7}$$

where ϵ is a small parameter. Since the nonlinear wave equations considered are autonomous, we can't *a priori* specify the period, we leave the period unspecified at this stage and introduce a new time variable, τ, with respect to which the sought-for periodic solution is 2π periodic. Let

$$t = \omega(\epsilon)^{-1}\tau, \ \omega(0) = \Omega, \tag{5.8}$$

and

$$b_1(t) = \beta_1(\tau), \ \beta_1(\tau + 2\pi) = \beta_1(\tau). \tag{5.9}$$

Then, equations (5.4-5.5) become:

$$\begin{aligned} \left(\omega^2(\epsilon)\partial_\tau^2 + \Omega^2\right)\beta_1(\tau) &= \epsilon\mathcal{F}_\beta(\beta_1, \eta_1; \epsilon) \\ \mathcal{F}_\beta(\beta_1, \eta_1; \epsilon) &\equiv -d^{-2}\langle \xi_\Omega, \mathcal{V}[\epsilon(\beta_1\xi_\Omega + \eta_1)](\beta_1\xi_\Omega + \eta_1)^2\rangle \end{aligned} \tag{5.10}$$

$$\begin{aligned} \left(\omega^2(\epsilon)\partial_\tau^2 + B^2\right)\eta_1(\tau, i) &= \epsilon\mathcal{F}_\eta(\beta_1, \eta_1; \epsilon) \\ \mathcal{F}_\eta(\beta_1, \eta_1; \epsilon) &\equiv -d^{-2}P_c\mathcal{V}[\epsilon(\beta_1\xi_\Omega + \eta_1)](\beta_1\xi_\Omega + \eta_1)^2 \end{aligned} \tag{5.11}$$

Let

$$\omega^2(\epsilon) = \Omega^2(1 + \epsilon\sigma(\epsilon)), \tag{5.12}$$

where $\sigma(\epsilon)$ is to be determined. Then (5.10) becomes

$$\left(\partial_\tau^2 + 1\right)\beta_1 = \frac{\epsilon}{1 + \epsilon\sigma(\epsilon)}[\sigma(\epsilon)\beta_1 + \Omega^{-2}\mathcal{F}_\beta(\beta_1, \eta_1; \epsilon)]. \tag{5.13}$$

We extract the leading order behavior by defining:

$$\beta_1 = \cos(\tau) + \epsilon\beta_2, \tag{5.14}$$

where

$$(\partial_\tau{}^2 + 1)\beta_2 = \frac{1}{1 + \epsilon\sigma(\epsilon)}[\sigma(\epsilon)\cos(\tau) + \epsilon\sigma(\epsilon)\beta_2 + \Omega^{-2}\mathcal{F}_\beta\left(\cos(\tau) + \epsilon\beta_2, \eta_1; \epsilon\right) \tag{5.15}$$

By the Fredholm alternative, equation (5.15) has an even 2π periodic solution if and only if

$$P_{\cos}(\sigma\cos(\tau) + \epsilon\sigma\beta_2 + \Omega^{-2}\mathcal{F}_\beta) = 0. \tag{5.16}$$

Here,

$$P_{\cos}\ g = \pi^{-1}\int_0^{2\pi}\cos(\mu)g(\mu)d\mu \tag{5.17}$$

is the projection onto the even 2π periodic null space of ∂_τ^2+1. The orthogonality constraint (5.16) can be rewritten as

$$\pi\sigma+\epsilon\sigma\int_0^{2\pi}\cos(\tau)\beta_2(\tau)d\tau+\omega_s^{-2}\int_0^{2\pi}\cos(\tau)\mathcal{F}_\beta\left(\cos(\tau)+\epsilon\beta_2(\tau),\eta_1;\epsilon\right)d\tau=0 \quad (5.18)$$

We have therefore reformulated the problem of finding a periodic solution of the discrete nonlinear wave equation, or equivalently (5.4-5.5), as the problem of finding 2π periodic solutions in τ, $(\beta_2(\epsilon),\eta_1(\epsilon),\sigma(\epsilon))$, of the system:

$$F(\beta_2,\eta_1,\sigma;\epsilon)=0, \quad (5.19)$$

where $F=(F_1,F_2,F_3)^t$, is defined by:

$$\begin{aligned} F_1(\beta_2,\eta_1,\sigma;\epsilon) &= (\partial_\tau^2+1)\beta_2 \\ -(1+\epsilon\sigma)^{-1}&\left[\sigma\cos(\tau)+\epsilon\sigma\beta_2+\Omega^{-2}\mathcal{F}_\beta\left(\cos(\tau)+\epsilon\beta_2,\eta_1;\epsilon\right)\right] \quad (5.20)\\ F_2(\beta_2,\eta_1,\sigma;\epsilon) &= \left(\Omega^2(1+\epsilon\sigma)\partial_\tau^2+B^2\right)\eta_1(\tau,i)-\epsilon\mathcal{F}_\eta(\cos(\tau)+\epsilon\beta_2,\eta_1;\epsilon) \\ & \quad (5.21)\\ F_3(\beta_2,\eta_1,\sigma;\epsilon) &= -(1+\epsilon\sigma)^{-1}\left[\pi\sigma+\epsilon\sigma\int_0^{2\pi}\cos(\tau)\beta_2 d\tau\right.\\ &\left.+\,\Omega^{-2}\int_0^{2\pi}\cos(\tau)\mathcal{F}_\beta(\cos(\tau)+\epsilon\beta_2(\tau),\eta_1;\epsilon)d\tau\right] \quad (5.22)\end{aligned}$$

We view F as a mapping of $(\zeta,\epsilon)\in\mathcal{X}\mapsto F(\zeta,\epsilon)\in\mathcal{Y}$. Here, $\mathcal{X}$ and $\mathcal{Y}$ are defined by:

$$\begin{aligned}\mathcal{X}\ :\ & \zeta=(\beta,\eta,\sigma) \text{ such that}\\ & \beta=\beta(\tau)\in H^2,\ \textit{even},\ \text{and } 2\pi \text{ periodic}\\ & \eta=\eta(\tau,\cdot)\in H^2\ \textit{even},\ \text{and } 2\pi \text{ periodic in } \tau\\ & \text{with values in the space of } \ l^2(\mathbb{Z}) \text{ functions and } \sigma\in\mathbb{R}\\ \mathcal{Y}\ :\ & \zeta=(\beta,\eta,\rho) \text{ such that}\\ & \beta=\beta(\tau)\in L^2,\ \textit{even},\ \text{and } 2\pi \text{ periodic}\\ & \eta=\eta(\tau,\cdot)\in L^2\ \textit{even},\ \text{and } 2\pi \text{ periodic in } \tau\\ & \text{with values in the space of } \ l^2(\mathbb{Z}) \text{ functions and}\\ & \rho=\int_0^{2\pi}\beta(\mu)\cos(\mu)d\mu.\end{aligned}$$

We find a particular $\zeta^{(0)}\in\mathcal{X}$ for which $F(\zeta^{(0)};0)=0$, and then seek to construct curve of solutions $\epsilon\mapsto\zeta(\epsilon)$, $\zeta(0)=\zeta^{(0)}$, for all sufficiently small ϵ using the implicit function theorem [44]. To find $\zeta^{(0)}$ we set $\epsilon=0$ and consider the system $F(\zeta;0)=0$. Taking $\eta_1=\eta_1^{(0)}\equiv 0$ and $\sigma=\sigma^{(0)}=0$, we find that $\beta_2^{(0)}$ satisfies the equation:

$$\left(\partial_\tau^2+1\right)\beta_2^{(0)}=-d^{-2}\Omega^{-2}\langle\xi_\Omega,\mathcal{V}[0]\xi_\Omega^2\rangle\cos^2(\tau), \quad (5.23)$$

which has the solution

$$\beta_2^{(0)}=-\frac{1}{2}d^{-2}\Omega^{-2}\langle\xi_\Omega\,\mathcal{V}[0]\xi_\Omega^2\rangle\left(1-\frac{1}{3}\cos(2\tau)\right). \quad (5.24)$$

Thus, $\zeta^{(0)} = (\beta_2^{(0)}, 0, 0) \in \mathcal{X}$ satisfies $F(\zeta^{(0)}; 0) = 0$. We shall now use the implicit function theorem to continue this solution to show that this solution deforms uniquely to nearby solutions for ϵ sufficiently small and nonzero.

To apply the implicit function theorem, it suffices to check that $d_\zeta F(\zeta^{(0)}; 0)$ is bounded and invertible. A computation yields:

$$d_\zeta F(\zeta^{(0)}; 0) = \begin{bmatrix} {\partial_\tau}^2 + 1 & 0 & -\cos(\tau) \\ 0 & \Omega^2 \partial_\tau^2 + B^2 & 0 \\ 0 & 0 & -\pi \end{bmatrix} \tag{5.25}$$

Invertibility of $d_\zeta F(\zeta^{(0)}; 0)$ can be shown by solving the system of inhomogeneous equations:

$$d_\zeta F \cdot \delta\zeta = R \tag{5.26}$$

where

$$\delta\zeta = \begin{bmatrix} \delta\beta_2 \\ \delta\eta_1 \\ \delta\sigma \end{bmatrix}, \quad R = \begin{bmatrix} B \\ E \\ \Sigma \end{bmatrix} \text{ and } \Sigma \equiv \int_0^{2\pi} \cos(\tau) B(\tau) d\tau. \tag{5.27}$$

The third equation implies:

$$\delta\sigma = -\pi^{-1}\Sigma. \tag{5.28}$$

Substitution into the first equation yields the equation an $\delta\beta_2$:

$$\left(\partial_\tau^2 + 1\right) \delta\beta_2 = B - \pi^{-1} \int_0^{2\pi} \cos(\mu) B(\mu) d\mu \ \cos(\tau), \tag{5.29}$$

which has an even 2π periodic solution. Finally the second equation can be rewritten as

$$(\Omega^2 {\partial_\tau}^2 + B^2)\delta\eta_1 = E = \sum_{n=0}^{\infty} \cos(n\tau) e_n \tag{5.30}$$

which can then be solved by Fourier series: $\delta\eta_1 = \sum_{n=0}^{\infty} g_n \cos(n\tau)$. We obtain

$$g_n = (B^2 - n^2\Omega^2)^{-1} e_n. \tag{5.31}$$

By **(NR)**, e_n is well-defined for each n. Note also that there is a strictly positive minimum distance of the set $\{n\Omega\}$ to $\sigma(B)$. Therefore,

$$\|g_n\|_{l^2(\mathbb{Z})} \leq \text{dist}\left((n\Omega)^2, \sigma(B^2)\right)^{-1} \|E_n\|_{l^2(\mathbb{Z})}, \tag{5.32}$$

from which we have boundedness of the inverse: $\left(\Omega^2 \partial_\tau^2 + B^2\right)^{-1}$:

$$\|\delta\eta_1\|_{H^2(\mathbb{R}; l^2(\mathbb{Z}))} \ \leq \ C\|E\|_{L^2(\mathbb{R}; l^2(\mathbb{Z}))}. \tag{5.33}$$

By the implicit function theorem there is a number $\epsilon_0 > 0$ such that for $\epsilon < \epsilon_0$ the nonlinear wave equation has a unique periodic solution of the form:

$$y_i(\tau, \epsilon) = K_i + (\epsilon\cos(\tau) + \epsilon^2\beta_2(\tau))\xi_{\Omega,i} + \epsilon\eta_1(i, \tau; \epsilon) \tag{5.34}$$

with $\tau = \omega(\epsilon)t$, $\omega^2(\epsilon) = \Omega^2(1+\epsilon\sigma(\epsilon))$ and β_2, η_1 2π periodic functions of τ. Note that $\eta_1 = \mathcal{O}(\epsilon)$, by the equation $F_2 = 0$, so that we have (5.1). This completes the proof of Theorem 5.1.

To prove Corollary 5.1, we note that by hypothesis, the direction of bifurcation is spatially odd. It is simple to check that the entire proof goes through with the spaces $\mathcal{X}$ and $\mathcal{Y}$ additionally constrained to consist of functions η, such that $\eta(\cdot, -i) = -\eta(\cdot, i)$.

5.2 Do quasiperiodic solutions bifurcate from the kink?

If we attempt using the above method of proof to construct quasiperiodic solutions, we do not succeed. To be specific, suppose we seek to construct a quasiperiodic solution which is generated by the two internal modes ξ_{Ω_1} and ξ_{Ω_1}. Formally, we seek $u_i(t) = u(i,t)$ in the form:

$$u(i,t) = K(i) + \epsilon \sum_{j=1}^{2} \alpha_j \xi_{\Omega_j}(i) \cos(\Omega_j t) + \epsilon \eta_1(i,t) \tag{5.35}$$

Substitution into the nonlinear wave equation gives

$$\begin{aligned} \left(\partial_t^2 + B^2\right)\eta_1 = \quad & -d^{-2}\epsilon\, \mathcal{V}\left[\epsilon \sum_{j=1}^{2} \alpha_j \xi_{\Omega_j} \cos(\Omega_j t) + \epsilon\eta_1\right] \\ & \times \left(\sum_{j=1}^{2} \alpha_j \xi_{\Omega_j} \cos(\Omega_j t) + \eta_1\right)^2 . \end{aligned}$$

Expansion of $\eta_1(i,t)$ as a power series in ϵ,

$$\eta_1(i,t) = \sum_{j=0}^{\infty} \epsilon^j \eta_1^{(j)}(i,t), \tag{5.36}$$

leads to a hierarchy of inhomogeneous equations of the form:

$$\left(\partial_t^2 + B^2\right)\eta_1^{(j)} = \mathcal{S}^{(j)}(t) \tag{5.37}$$

where as j increases $\mathcal{S}^{(j)}(t)$ contains a finite sum of terms with time-frequencies of the form $n_1\Omega_1 + n_2\Omega_2$ with $|n_1| \le N_1^{(j)}$, $|n_2| \le N_2^{(j)}$ and $N_1^{(j)}$, $N_2^{(j)}$ increasing with j. Thus it is natural to solve for each $\eta_1^{(j)}$ as a truncated multiple Fourier series:

$$\eta_1^{(j)} = \sum_{|n_1| \le N_1^{(j)}, n_2 \le N_2^{(j)}} e^{i(n_1\Omega_1 + n_2\Omega_2)t} g_{n_1,n_2}^{(j)}. \tag{5.38}$$

Substitution into (5.37) yields:

$$\left(B^2 - (n_1\Omega_1 + n_2\Omega_2)^2\right) g_{n_1,n_2}^{(j)} = \mathcal{G}_{n_1,n_2}^{(j)}, \tag{5.39}$$

where $\mathcal{G}^{(j)}_{n_1,n_2}$ denotes the term in $\mathcal{S}^{(j)}(t)$ which is proportional to $\exp(i(n_1\Omega_1+n_2\Omega_2)t)$. In order to ensure the general solvability of (5.39) we need that for any $n_1, n_2 \in \mathbb{Z}$,

$$n_1\Omega_1 + n_2\Omega_2 \;\notin\; \pm\sigma(B). \tag{5.40}$$

Although it is nongeneric for a frequency in the point spectrum (internal mode frequency) to be hit, since the continuous spectrum (phonon band) is an interval, generically one has $n_1\Omega_1 + n_2\Omega_2 \in \sigma_{cont}(B)$, for infinitely many choices of n_1, n_2. For such choices the operator on the right hand side of (5.39) is not invertible and these resonant frequencies are an obstruction to solvability. A closer look at the set of resonances and their contribution on the dispersive normal form, would give insight into the *lifetime* of such eventually decaying quasiperiodic oscillations.

6 Large time behavior in a neighborhood of K_{gs}

In this section we combine the normal form analysis of section 4, and the existence theory for time periodic solutions of section 5 with numerical simulation to get a more detailed picture of the large time behavior of discrete ϕ^4 and SG in a neighborhood of the ground state kink. We shall make repeated use of Tables 2 and 4 for ϕ^4 and of Tables 6 and 7 for SG in which the normal form / power equations and coherent structures are tabulated. In interpreting these tables we recall that ε, introduced in (3.5), measures the size of the component of the perturbation about the kink in the internal mode subspace. In full simulations of the evolution equation ε is typically of order 10^{-1}, and therefore some of the decay phenomena anticipated by our analysis, occur on very large time scales (*e.g.* $\tau \sim \varepsilon^{-2}, \varepsilon^{-4}$ or longer) and are difficult to simulate accurately.

In each of the various $d-$ ranges we proceed as follows: we mention the relevant coherent structures (the high energy kink is omitted because it is unstable). These are all anticipated by the normal form analysis and their existence is established rigorously in section 5. We then discuss the numerically observed large time behavior for different classes of initial conditions. This gives evidence of the attracting nature of the periodic solutions constructed in section 5 in various regimes of the discreteness parameter d.

As mentioned in the introduction, this is related to the final stages of the evolution of a propagating kink, pinned to a particular lattice site, and its damped oscillation to an asymptotic state within the Peierls-Nabarro potential.

6.1 Discrete ϕ^4

Regimes II, III and V: The coherent structures of interest are: K_{gs} and W. Numerical simulations show that the wobbling kink, W, is a local attractor.
Regimes I,IV: The coherent structures of interest are: K_{gs} , W and gW.

Experiment 1 (data given by K_{gs} plus a small multiple of the Goldstone (even) g-mode): solution appears to approach gW.

Experiment 2 (data given by K_{gs} plus a small multiple of the shape (odd) s-mode): solution appears to approach W.

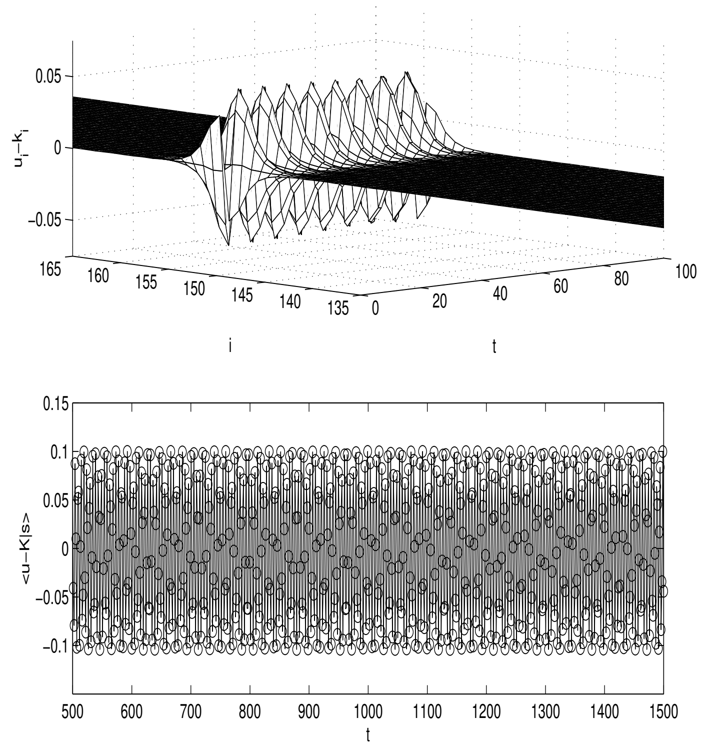

Figure 8: Simulation of discrete ϕ^4 with $d = 0.8$ in Regime IV. Upper panel: $u(t) - K_{gs}$ is seen to be approximately equal to the (spatially odd) shape mode. Lower panel: Projection of $u(t) - K_{gs}$ onto the shape mode, s; principal frequency of oscillation is approximately ω_s

Experiment 3 (data given by a general small perturbations of K_{gs}): gW and W appear to have basins of attraction. Although an exact determination of this basin is not analytically tractable, its projection onto the internal mode subspace, the span of $\{g, s\}$, can be approximated using the internal mode power equations and the explicit information on coefficients from Table 1. In particular, we find

$$\frac{dQ}{dP} = \frac{\omega_g}{\omega_s} \tag{6.41}$$

from which one gets the prediction that for data with

$$|B(0)|^2 < \frac{\omega_g}{\omega_s}|A(0)|^2, \tag{6.42}$$

solutions asymptotically approach a *g-wobbler*, gW, while for

$$|B(0)|^2 > \frac{\omega_g}{\omega_s}|A(0)|^2, \tag{6.43}$$

solutions asymptotically approach a *wobbler*, W.

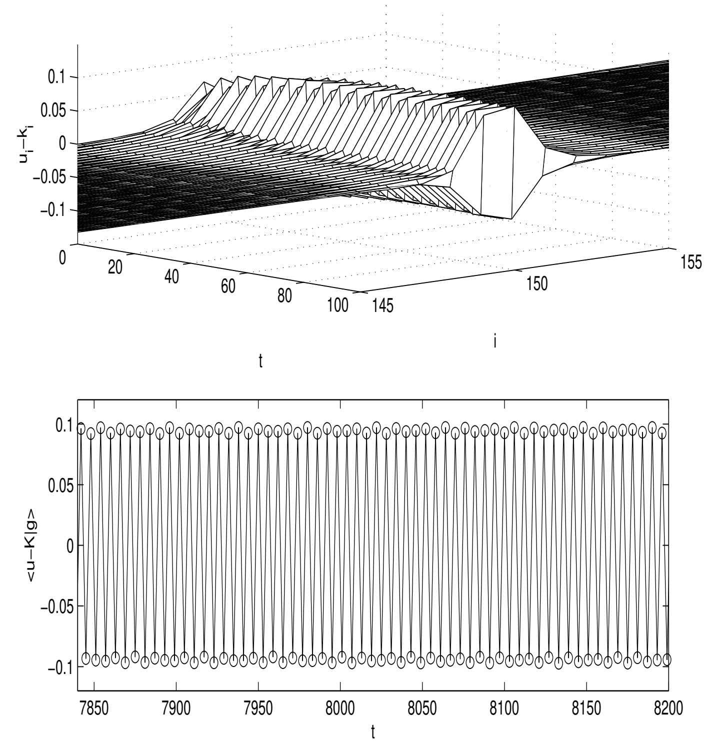

Figure 9: Simulation of discrete ϕ^4 with $d = 0.65$ in Regime IV. Upper panel: $u(t) - K_{gs}$ is seen to be approximately equal to the (spatially even) Goldstone mode, g. Lower panel: Projection of $u(t) - K_{gs}$ onto the Goldstone mode; principal frequency of oscillation is approximately ω_g.

Regime VI: The phase portrait of the normal form jumps from dimension 2 to dimension 3 due to the appearence of a (spatially even) edge mode. In addition to the ground state kink, K_{gs}, there are time-periodic (wobbling solutions) W and eW. Numerical simulations indicate the presence of very long lived quasiperiodic oscillations about the kink. These appear to be oscillations of the form represented in the first two terms of (5.35). Strong evidence of the eventual decay of such oscillations can be seen as follows:

- In section 5.2 we have shown that an attempt to construct quasiperiodic solutions breaks down due to a high order resonance, *i.e.* $n_1\omega_s + n_2\omega_e \in \sigma_{cont}(B)$, where $|n_1| + |n_2|$ is large. In this particular case, we have $-\omega_s + 2\omega_e \in \sigma_{cont}(B)$; see Table 2.

- Such resonances correspond to obstructions in the power equations to equilibrium solutions of the form: $(0, Q, R)$ with both Q and R nonzero. The obstructing term is the term $-\varepsilon^4 QR^2$ in the R equation.

- Linearization of the power equations about any equilibrium point $(0, Q_{eq}, 0)$ or $(0, 0, R_{eq})$ shows that each line of equilibria is asymptotically stable, corresponding to the conclusion that quasiperiodic oscillations will damp with a resulting asymptotically periodic state, W or eW, depending on initial conditions. The time scale of decay of these oscillations, τ, is set by the order in ε of the obstructing terms, *e.g.* $\tau \sim \varepsilon^{-4}$.

Regime VII: The coherent structures of interest are: K_{gs} and eW.
Experiment 1: For data which is an odd perturbation of K_{gs}. K_{gs} is the attractor.
Experiment 2: For general data, eW appears to be a local attractor.
Regime VIII: The coherent structure of interest is K_{gs}.
Experiment 1 (data given by K_{gs} plus an small perturbation in the direction of the (odd) shape mode): approach to K_{gs} at a rate $\mathcal{O}(t^{-\frac{1}{2}})$.
Experiment 2 (data given by K_{gs} plus an small perturbation in the direction of the (even) edge mode): approach to K_{gs} at a rate $\mathcal{O}(t^{-\frac{1}{2}})$.
Experiment 3 (data given by K_{gs} plus an small perturbation in the direction of the (even) Goldstone mode): perturbation from K_{gs} appears to decay but at a different rate and on much longer time scales than in Experiments 1 and 2.

6.2 Discrete sine-Gordon

Following the model of the previous subsection, we indicate relevant coherent structures and briefly discuss the dynamics in a neighborhood of the ground state kink for the discrete sine-Gordon equation.
Regime I: The coherent structures of interest are: K_{gs} and gW. For general data, gW appears to be a local attractor.
Regime II: The coherent structures of interest are: K_{gs}, W and gW. The dynamical behavior is as, for example, in regime IV for the ϕ^4 model.
Regime III: The coherent structures of interest are K_{gs} and W. Numerical simulations show that W is a local attractor.

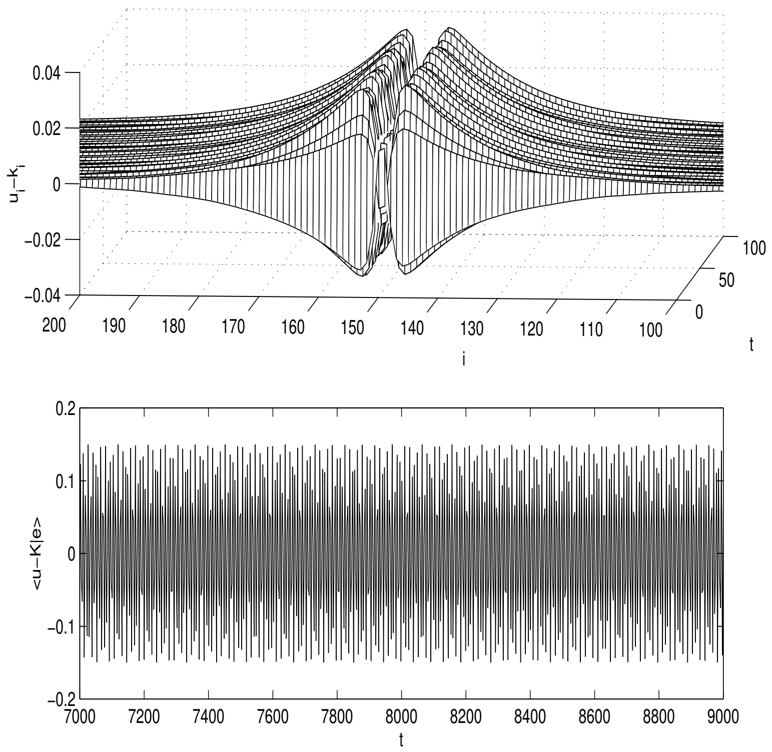

Figure 10: Simulation of discrete ϕ^4 with $d = 1.1$ in Regime IV. Upper panel: $u(t) - K_{gs}$ is seen to be approximately equal to the (spatially even) edge mode, e. Lower panel: Projection of $u(t) - K_{gs}$ onto the edge mode; principal frequency of oscillation is approximately ω_e.

Regime IV: For all $d \geq d_*$, there are positive integer multiples of both ω_g and ω_e which fall in the phonon band, $\sigma_{cont}(B)$. Therefore, hypothesis **(NR)** of section 5 is not satisfied for either internal mode, and the existence theory of periodic solutions breaks down. A general perturbation about K_{gs} will excite the internal modes and these resonances are responsible for transfer of energy from the internal modes to K_{gs} and to radiation modes. The asymptotic state is observed to the ground state kink, with the details of the damped oscillatory approach to it, being predicted by the various $d-$ dependent normal forms.

Within each subregime of regime IV, the power equations are, up to terms which can be shown to be negligible for large t, of the form

$$\begin{aligned} P_t &= -\varepsilon^{2n} P^n \\ Q_t &= -\varepsilon^2 PQ. \end{aligned}$$

It follows that

$$P(t) = P_0(1 + (n-1)P_0^{n-1}\varepsilon^{2n}t)^{-\frac{1}{n-1}} \tag{6.44}$$

and that $Q(t)$ is decaying at exponentially. These predicted power laws for $P(t)$ (on a time scale of order ε^{-2n}, and the implied very rapid decay of Q are, to a good degree of approximation, observed in numerical simulations of the discrete sine-Gordon equation. In particular, using the form of the near-identity transformation (4.24), we obtain for the decay rates (of initial conditions with general data):

- $0.86 \sim d_* \leq d < 0.9$: $n = 3$, $P(t) = \mathcal{O}(t^{-\frac{1}{2}}) \rightarrow |a(t)|, |b(t)| \sim \mathcal{O}(t^{-\frac{1}{4}})$
- $0.9 \leq d < 0.99$: $n = 4$, $P(t) = \mathcal{O}(t^{-\frac{1}{3}}), \rightarrow |a(t)|, |b(t)| \sim \mathcal{O}(t^{-\frac{1}{6}})$
- $0.99 \leq d < 1.003$: $n = 5$, $P(t) = \mathcal{O}(t^{-\frac{1}{4}}), \rightarrow |a(t)|, |b(t)| \sim \mathcal{O}(t^{-\frac{1}{8}})$

Note, however, that for purely odd initial perturbations around the ground state kink in this regime, the edge mode projection decays as $t^{-1/2}$, as dictated by the $-\varepsilon^2 Q^2$ term.

7 Summary and open questions

Summary: In this paper we have considered the large time behavior of solutions to discrete nonlinear wave equations, particularly the discrete sine-Gordon and discrete ϕ^4 models, for initial conditions which are a small perturbation of a stable (ground state) kink.
(1) We have proved in the regime where the discreteness parameter is sufficiently small, corresponding to sufficiently large lattice spacing or weak coupling of neighboring oscillators, the existence of various classes of time periodic solutions. These include the, in the case of the ϕ^4 the wobbling kinks (W), which have the same spatial symmetry as the kink, and which were anticipated in previous numerical studies as well as e-wobblers (eW) and g-wobblers (gW), periodic solutions which do not respect the spatial symmetry of the kink. In the SG case, it is the eW's that respect the spatial symmetry while the gW's do not.

(2) We have used the methods of scattering theory and (Hamiltonian dispersive) normal forms to study the final stages of pinning of a kink to a particular lattice site. For large values of the discreteness parameter ("near" the continuum regime), the asymptotic state is a static kink. In contrast, for small values of the discreteness parameter, the above time periodic states can be attracting orbits. This is in sharp contrast to the behavior of solutions for the corresponding continuum equation in which a (possibly moving) kink is the attractor. Our analysis makes clear the relation of broken (Lorentz) invariance to these contrasting dynamics. Our results give a systematic clarification of the physicist's heuristic picture of the dynamics of the center of mass of the kink as the effective (radiation-) damped motion of a massive particle in the Peierls-Nabarro potential. The approach to asymptotic state is via a slow damped (periodic or quasiperiodic) oscillation. The damping of the oscillation can indeed be very, very slow, and the *lifetime* is deducible from the normal form.

The methods we use are very systematic and general, and apply to many situations [51, 52, 53] where the dynamical system can be viewed as the interaction of two subsystems: a finite dimensional subsystem, here governing the kink and its internal oscillations, and an infinite dimensional dynamical system, here governing dispersive radiation. In particular, one problem of related interest in which these methods can be readily generalized is the behavior of pulse-like breathing modes in the discrete non-linear Schrödinger equation $i\psi_{i,t} = -k\delta^2\psi_i - |\psi_i|^2\psi_i$. Time periodic and spatially localized states can be found in the form: $\psi_i = \exp(\sqrt{-1}\omega t)u_i$. In an appropriate limit, breather solutions of nonlinear equations can be constructed from these; see, for example, [58]. Lyapunov stability of such states (see for example footnote 6 in section 2) is established in [58]. This notion of stability, being defined in terms of conserved integrals, is insensitive to the radiative behavior and the asymptotic approach to a ground state. For a recent account of the (numerical) construction and stability of such modes, see for instance [32]. The techniques of this paper apply directly to the study of dispersive waves and the radiation losses from internal modes of the pulse-like coherent structure. Related formal asymptotic methods are used to study such effects in [45, 46].

Open questions: There are many related open problems of which we now mention several.

- Although the normal form analysis anticipates the existence and stability properties of various time-periodic solutions, we only have a rigorous theory concerning their existence. Linear stability theory would require an infinite dimensional Floquet analysis, and nonlinear stability theory would require the analogue of our normal form in a neighborhood of a periodic, rather than static, solution. Numerically, the asymptotic stability of the time periodic structures can be concluded from their persistence for long time integrations (to the extent of our computational power). The periodic structure construction and stability can also be performed using a limit-cycle type of technique similar to the one considered in [2, 40]. The rigorous stability theory however is still a challenging open problem.

- A rigorous infinite time theory, as in [53], for discrete nonlinear wave equations with kinks is a challenging open question. The problem is challenging even in the continuum case, where the kink is the sole attractor. In this case, the normal form yields the correct asymptotic rate of decay [39, 49]. However, due to the strength of the interaction (in space dimension one) of the dispersive and bound state components, the deviation of the full solution, $u(t)$, from the kink plus its internal mode modulations is **not** asymptotically free, *i.e.* not a free dispersive solution of the linear Klein-Gordon equation. Rather, it requires a solution-dependent logarithmic in time corrected phase [49], characteristic of long range scattering problems.

- Of interest would be more detailed long time simulations which would further elucidate the large time dynamics and assist in mapping out basins of attraction for various periodic states.

- Our study gives a detailed picture of the final stages of the pinning of a kink to a particular lattice site. However, the early stages of a kink plus *large* perturbation propagating in a lattice have some of the same features of the regime we consider. Namely [48], as the kink's center of mass moves under the influence of the Peierls-Nabarro potential, it executes repeated acceleration and slowing with an approximate PN frequency. This oscillation appears to resonate with continuous radiation modes, resulting in an emission of energy, deceleration of the kink and eventual capture of the kink by a particular lattice site. It would be of interest to extend and apply the ideas of the current paper to this problem.

- In this paper we have analyzed the problem of radiative effects of discreteness for the $2-\pi$ kinks within the P-N barrier (for a recent review on the effects of discreteness as well as the physical applications of a number of models similar to the ones considered here see [6]). It is well-known however that in the SG lattices multiple kinks ($2n\pi$ kinks in general) can also exist. For these kinks first mentioned in [48] the static stability picture was analyzed in [3]. There are a number of open problems regarding the behavior of such modes:

  1. Their motion prior to pinning is only very slightly effected by radiative phenomena [48]. This phenomenon hasn't been accounted for satisfactorily to the best of our knowledge to date. In fact, this forms a part of a more general problem concerning the motion of coherent structures in lattices. It is known that under certain conditions and for potential different than the ones considered here [12, 26] there exist lattice systems with travelling wave solutions. Hence, it would be very interesting to elucidate the general conditions under which such lattice systems support travelling wave solutions (or equivalently under which conditions solutions to the advance-delay equations of the travelling wave frame exist).

  2. When trapped (eventually) in the PN barrier these moving $4-\pi$ kinks also radiate in a way that can be captured by the analysis of this paper. The problem there will have more (as shown in [3]) internal modes bifurcating

from the continuum and hence will be more complicated but it can still be analyzed in the way presented above.

Acknowledgements

Thanks are expressed to N.J. Balmforth, A.R. Bishop, J.L. Lebowitz, C.K.R.T. Jones, Y.G. Kevrekidis, H. Segur and A. Soffer for stimulating discussions and for suggesting some important references. P.G.K. gratefully acknowledges assistanship support from the Computational Chemodynamics Laboratory of Rutgers University, fellowship support from the "Alexander S. Onasis" Public Benefit Foundation and also partial support from DIMACS.

References

[1] W. Atkinson, N. Cabrera *Phys. Rev. A*, **138**, 763, 1965

[2] S. Aubry *Physica D*, **103**, 201, 1997

[3] N.J. Balmforth, R.C. Craster, P.G. Kevrekidis *Physica D*, **135**, 212,2000

[4] A.R. Bishop, S.E. Trullinger, J.A. Krumhansl *Physica D*, **1**, 1, 1980

[5] L. Bonilla & J.B. Keller, *J. Stat. Phys.*, **42** 1115-1125, 1986

[6] O.M. Braun, Yu. S. Kivshar *Phys. Rep.*, **306**, 1, 1998

[7] O.M. Braun, Yu. S. Kivshar, M. Peyrard *Phys. Rev. E*, **56**, 6050, 1997

[8] R. Boesch, P. Stancioff, C.R. Willis *Phys. Rev. B*, **38**, 6713, 1988

[9] R. Boesch, C.R. Willis *Phys. Rev. B*, **42**, 6371, 1990

[10] R. Boesch, C.R. Willis, M. El-Batanouny *Phys. Rev. B*, **40**, 2284,1989

[11] R. Boesch, C.R. Willis *Phys. Rev. B*, **39**, 361, 1989

[12] J.W. Cahn, J. Mallet-Paret, E.S. Van Vleck *SIAM J. Appl. Math.*, **59**, 455, 1998

[13] J. Carr, Applications of Center Manifold Theory, Applied Mathematical Sciences, Volume 35, Springer Verlag, New York-Berlin, 1981

[14] E. Coddington & N. Levinson, Theory of Ordinary Differential Equations, Mc-Graw Hill, New York 1955

[15] J.A. Combs, S. Yip *Phys. Rev. B*, **28**, 6873, 1983

[16] J.F. Currie, S.E. Trullinger, A.R. Bishop, J.A. Krumhansl *Phys. Rev. B*, **15**, 5567, 1977

[17] T. Dauxois *Phys. Lett. A*, **159**, 390 1991.

[18] T. Dauxois, M. Peyrard, A.R. Bishop *Physica D*, **66**, 35, 1993

[19] T. Dauxois, M. Peyrard, C.R. Willis *Physica D*, **57**, 267, 1992

[20] P.G. Drazin, Solitons, *Cambridge University Press*, 1983.

[21] H.S. Eisenberg, Y. Silberberg, R. Morandotti, A.R. Boyd & J.S. Aitchison, *Phys. Rev. Lett.* **81**, 3383, 1998.

[22] J. Frenkel, T. Kontorova *J. Phys. USSR* , **1** 137, 1939.

[23] J.H. Heiner *Phys. Rev. A*, **136**, 863, 1964.

[24] D.B. Henry, J.F. Perez & W.F. Wreszinski, Comm. Math. Phys. **85**, 351–361, 1982

[25] T. Holst, L.E. Guettero, N. Gronbech-Jensen, J.A. Blackburn, J. Bindlev-Hansen in Superconducting Devices and their Applications, Springer-Verlag, 1992.

[26] G. Iooss, K. Kichgassner, Travelling waves in a chain of coupled nonlinear oscillators, (preprint), 1999

[27] Y. Ishimori, T. Munakata *J. Phys. Soc. Japan*, **51**, 3367, 1982

[28] P.G. Kevrekidis, C.K.R.T. Jones, T. Kapitula, Exponentially small splitting of heteroclinic orbits: from the rapidly forced pendulum to discrete solitons, *Phys. Lett. A*, submitted, 2000.

[29] J.P. Keener, D.W. McLaughlin *Phys. Rev. A*, **16**, 777, 1977

[30] P.G. Kevrekidis *GFD 1998 Summer School Proceedings*, WHOI, 1999 (available at http://www.whoi.edu/gfd/)

[31] P.G. Kevrekidis, C.K.R.T. Jones, Bifurcation of internal solitary wave modes from the essential spectrum, *Phys. Rev. E*, to appear, 2000

[32] P.G. Kevrekidis, K.Ø. Rasmussen, A.R. Bishop Localized excitations and their thresholds, *Phys. Rev. E*, to appear, 2000

[33] E. Kirr, M.I. Weinstein, Parametrically excited Hamiltonian Partial Differential Equations, submitted, 1999

[34] Yu. S. Kivshar, D.E. Pelinovsky, T. Cretegny, M. Peyrard *Phys. Rev. Lett.*, **80**, 5032, 1998

[35] H. Lamb *Proc. Lond. Math. Soc.* **32** 208–211, 1900

[36] L.D. Landau, E.M. Lifschitz, Quantum Mechanics, Reading, MA: Addison-Wesley, 1958.

[37] J.L. Lebowitz *J. Phys. A*, **194**,1, 1993

[38] R. S. MacKay, S. Aubry *Nonlinearity*, **7**, 1623, 1994

[39] N. Manton & H. Merabet, *Nonlinearity*, **10**, 3, 1997

[40] P.J. Martinez, L.M. Floria, J.L. Marin, S. Aubry, J.J. Mazo *Physica D*, **119**, 175, 1998

[41] D.W. McLaughlin, A.C. Scott *Phys. Rev. A*, **18**, 1652, 1978

[42] P.D. Miller, A. Soffer & M.I. Weinstein, Metastability of breather modes of time dependent potentials, *Nonlinearity*, to appear, 2000.

[43] R. Morandotti, U. Peschel, J.S. Aitchison, H.S. Eisenberg & Y. Silberberg, *Phys. Rev. Lett.* **83** 2726–2729, 1999

[44] L. Nirenberg, Topics in Nonlinear Functional Analysis, Courant Institute Lecture Notes, 1974

[45] D.E. Pelinovsky, V.V. Afanasjev, Yu.S. Kivshar *Phys. Rev. E*, **53**, 1940, 1996

[46] D.E. Pelinovsky *Physica D*, **119**, 301, 1998

[47] M. Peyrard, S. Aubry, *J. of Phys. C*, **16**, 1593, 1983

[48] M. Peyrard, M.D. Kruskal *Physica D*, **14**, 88, 1984

[49] R. Pyke, A. Soffer & M.I. Weinstein, (in preparation).

[50] H. Segur *J. Math. Phys.*, **24**, 1439, 1983

[51] A. Soffer, M.I. Weinstein *Geome. func. anal. - GAFA*, **8**, 1086–1128, 1998

[52] A. Soffer, M.I. Weinstein *Journal of Statistical Physics*, **93**, 359-390, 1998

[53] A. Soffer, M.I. Weinstein *Inventiones Mathematicae*, **136**, 9–74, 1999

[54] P. Stancioff, C. Willis, M. El-Batanouny, S. Burdick *Phys. Rev. B*, **33**, 1912, 1986

[55] A.V. Ustinov, T. Doderer, I.V. Vernik, N.F. Pedersen, R.P Huebener, V. A. Oboznov *Physica D*, **68**, 41 1994

[56] M.I. Weinstein, *Rocky Mtn. J. Math.* **21**, 821–827, 1991

[57] M.I. Weinstein, *Contemp. Math.* **200**, 223-235, 1996

[58] M.I. Weinstein *Nonlinearity*, **12** 673, 1999

[59] C. Willis, M. El-Batanouny, P. Stancioff *Phys. Rev. B*, **33**, 1904, 1986

[60] K. Xu,D. Lu,X. Yao *The Chinese Journal of Low Temperature Physics*, **14**, 293, 1992.

[61] X. Yang, Y. Zhuo, X. Wu *Phys. Lett A*, **234**, 152, 1997.